

# Further Evaluation of a Hearing Loss Simulator

by

David Soleau Lum

Submitted to the Department of Electrical Engineering and Computer Science  
in partial fulfillment of the requirements for the degree of

Master of Engineering in Electrical Engineering and Computer Science

at the

MASSACHUSETTS INSTITUTE OF TECHNOLOGY

June 1995

©David Soleau Lum, 1995. All rights reserved.

The author hereby grants to MIT permission to reproduce and distribute publicly  
paper and electronic copies of this thesis document in whole or in part, and to grant  
others the right to do so.



Author.....  
Department of Electrical Engineering and Computer Science  
May 30, 1995

Certified by ..  
Louis D. B. Braida  
Henry Ellis Warren Professor of Electrical Engineering  
Thesis Supervisor



Accepted by.....  
Frederic R. Morgenthaler  
Chairman, Department Committee on Graduate Theses

MASSACHUSETTS INSTITUTE  
OF TECHNOLOGY

AUG 10 1995

LIBRARIES  
Barker Eng

# Further Evaluation of a Hearing Loss Simulator

by

David Soleau Lum

Submitted to the Department of Electrical Engineering and Computer Science  
on May 30, 1995, in partial fulfillment of the  
requirements for the degree of  
Master of Engineering in Electrical Engineering and Computer Science

## Abstract

A real-time, level-expansion system to simulate hearing loss for normal hearing persons was studied. The simulator's effect on the performance of normal hearing subjects in basic psychoacoustic tasks was investigated through experimentation. The experiments performed included measurements of intensity discrimination, critical ratio, and two-tone suppression. The results of these experiments were predicted by analyzing a model of the simulator system. The results of a psychophysical tuning curve (PTC) experiment were also predicted and compared with previous data. In addition to the expansion simulation, an additive noise based simulation of hearing loss (equivalent threshold masking) was investigated in each experiment. Results show that the noise and expansion simulations produce comparable effects that are similar to the effects of a real impairment in the PTC and critical ratio experiments. In the intensity discrimination experiment, the expansion simulation gave subjects abnormally good sensitivity, which is not associated with real impairment.

Software meant to increase the precision and ease of use of the expansion simulator and stimulus generation equipment was written and documented.

Thesis Supervisor: Louis D. B. Braida

Title: Henry Ellis Warren Professor of Electrical Engineering

## Acknowledgments

Most importantly, I would like to thank my parents, Jennifer and Martin Lum. You two have been the best parents a guy could hope for! You have instilled in me morality, self-respect, and the desire to learn, which I consider to be my most valuable assets. I never could have succeeded in graduate school without your years of unconditional love and support.

To my fiancé, Alyssa: you have always been there for me in the past five years, and I pledge to always be there for you in the next hundred. You have given me a solid target to aim for in the past year, and I never would have finished on time had there not been a better life waiting in the wings, urging me on.

To my twin, John: I would say that “I’ve leaned on you more than you know” in the past few years, but that wouldn’t be accurate. I think you understand perfectly well how much we’ve leaned on each other throughout our lives. It’s been great rooming with you this year, even if your monstrous television nearly caused my academic downfall.

To my advisor, Lou: you have been far more than a thesis advisor during our lengthy acquaintance. You’ve probably had a better vantage point than anyone else to watch me mature, and I have relied heavily on your advice and generosity. My catching you as a friend lends more credence to the theory that I am the luckiest person on earth. (There. I didn’t even mention the word “wavelets.”)

I am indebted to my subjects: JL, KL, AM, and JW. They endured long hours in the isolation of a soundproof booth, but they did it with great enthusiasm.

Finally, thanks to the members of the Friday Afternoon Club: Joe, Jeanie, Maroula, Paul, Phil, Jay, Matt, Mike, Louise, and Zulfiqar. It’s been good fun.

# Contents

<b>1</b>	<b>Introduction</b>	<b>12</b>
1.1	Background . . . . .	12
1.1.1	Psychoacoustics . . . . .	12
1.1.2	Hearing Loss . . . . .	13
1.1.3	Hearing Loss Simulation . . . . .	15
1.2	Goals . . . . .	18
<b>2</b>	<b>Software Development</b>	<b>20</b>
2.1	Laboratory Setup . . . . .	20
2.2	Low-level Software . . . . .	21
2.2.1	Purpose . . . . .	21
2.2.2	Implementation . . . . .	22
2.3	High-level Software . . . . .	23
2.3.1	Purpose . . . . .	23
2.3.2	Implementation . . . . .	23
2.4	Documentation . . . . .	23
<b>3</b>	<b>Experiments</b>	<b>24</b>
3.1	Intensity Discrimination . . . . .	24
3.1.1	Experimental Parameters . . . . .	25
3.2	Psychophysical Tuning Curves . . . . .	26
3.2.1	Neural Tuning Curves . . . . .	26
3.2.2	Psychophysical Tuning Curves . . . . .	27
3.2.3	Experimental Parameters . . . . .	28
3.3	Simultaneous Masking . . . . .	28
3.3.1	Experimental Parameters . . . . .	30
3.4	Two Tone Suppression . . . . .	30
3.4.1	Experimental Parameters . . . . .	31

<b>4</b>	<b>Modelling and Predictions</b>	<b>32</b>
4.1	Intensity Discrimination . . . . .	32
4.2	Psychoacoustic Tuning Curves . . . . .	37
4.3	Simultaneous Masking . . . . .	42
4.3.1	Two Tone Suppression . . . . .	49
<b>5</b>	<b>Experimental Results</b>	<b>50</b>
5.1	Intensity Discrimination . . . . .	50
5.2	Psychophysical Tuning Curves . . . . .	54
5.3	Simultaneous Masking . . . . .	55
5.4	Two Tone Suppression . . . . .	57
<b>6</b>	<b>Discussion</b>	<b>61</b>
6.1	Intensity Discrimination . . . . .	61
6.2	Psychoacoustic Tuning Curves . . . . .	62
6.3	Simultaneous Masking . . . . .	62
<b>7</b>	<b>Conclusion</b>	<b>65</b>
<b>A</b>	<b>Derivation of Sensitivity-per-Bel Measures from Experimental Data</b>	<b>68</b>

# List of Figures

1-1	Schematized results of a loudness balancing experiment with a normal subject (left), a subject with a monaural pure conductive loss (middle), and a subject with a monaural pure sensorineural loss. (right). The “ $\Delta$ ” symbols indicate points of equal loudness. Roughly speaking, the degree of hearing loss is given by the difference $X$ . . . . .	14
1-2	Recruitment in monaurally impaired subjects. At conditions of equal loudness, the $x$ ’s plot intensity of tones in the normal ears (vertical axis) versus intensity of tones in the impaired ears (horizontal axis). This figure is from Miskolczy-Fodor, 1960. . .	15
1-3	Loudness balancing curve reinterpreted as a simulator input/output function. The solid line is the input/output function, with a reference gain of unity indicated by the dashed line. Normal threshold is marked $T_n$ , impaired threshold as $T_i$ , and the threshold of complete recruitment as $T_r$ . . . . .	17
2-1	Original laboratory setup for psychoacoustics experiments in the author’s AUP. Note the noisy analog channel between DSP boards. . . . .	21
2-2	New laboratory setup, improved due to much new software and some new hardware.	22
3-1	Effects of the expansion simulator on the intensity discrimination stimuli. At the input, tone bursts are separated by a small intensity difference. At the output, the difference in intensity is exaggerated and the overall level has been reduced. . . . .	25
3-2	Comparison of a neural tuning curve from an undamaged cochlea (dashed line) with an NTC from a cochlea whose inner and outer hair cells had both been damaged (solid line). Liberman and Dodds, 1984. . . . .	26
3-3	A schematic of the stimulus in a forward-masked PTC experiment. A short, quiet probe tone is presented shortly after a longer, more intense masker tone. . . . .	27
3-4	Use of a broadband masker and a narrow band probe to measure the bandwidth of an auditory filter. . . . .	28

3-5	Comparison of the stimulus used in the PTC experiment with the stimulus used in the suppression experiment. In the suppression experiment, the masker intensity is fixed and the probe threshold $T$ is measured. Adding a suppressor tone to the masker can actually <i>lower</i> the threshold of the probe to $T_S$ . . . . .	30
4-1	Intensity discrimination of an average normal hearing subject, measured in sensitivity-per-Bel as a function of sensation level (decibels above threshold). The stimulus is a long-duration pure tone at 1 kHz. Taken from Rabinowitz et al. (1976). . . . .	33
4-2	Algorithm to predict expansion-simulated intensity discrimination. . . . .	34
4-3	Comparison of predicted intensity discrimination in the expansion simulated condition with data from normal hearing persons from Rabinowitz et al. The comparisons are made for stimuli at equal sound pressure level, with simulated losses of 20, 30, 40, and 50 dB. The dashed lines reproduce the normal data from Figure 4-1, and the solid lines are the predicted functions from the expansion simulated condition. At the top of each panel is the simulator expansion factor $K$ . . . . .	35
4-4	Same data as in Figure 4-3 compared at equal <i>sensation levels</i> rather than equal sound pressure levels. . . . .	36
4-5	Same data as in Figure 4-3 compared at equal <i>loudness</i> rather than equal sound pressure levels. The simulator's static input/output function was used to determine points of equal loudness in the unsimulated and expansion simulated conditions. . .	36
4-6	The psychophysical tuning curve, as a function of both masker frequency and probe level. Probe levels and frequency are indicated with the "◇" symbols. As the probe level increases, so does the height and broadness of the tuning curve. . . . .	37
4-7	Algorithm for predicting the PTC experiment for normal-hearing subjects using the expansion hearing loss simulation. . . . .	38
4-8	Tuning curves from a hypothetical normal-hearing subject using the expansion simulator with a variety of flat losses. The dotted line at bottom is the subject's normal threshold. The solid line is the subject's normal tuning curve, and the dashed lines represent PTCs at simulated losses of 20, 30, 40, and 50 dB. The ◇ symbols indicate the frequency and level of the probe, which is always 10 dB above the (impaired) threshold. The curves were calculated using the method of Figure 4-7. . . . .	39
4-9	Static input/output relations are shown for hearing losses of 0 through 50 dB. At each degree of loss, an input tone of 10 dB SL (10 dB above impaired threshold) is mapped from the input to the output, shown with dotted lines. Although the input level is maintained at 10 dB above threshold, the output level increases with the degree of hearing loss. . . . .	40

4-10	Predictions of expansion simulated tuning curves using the appropriate probe tone input level in each condition to ensure that the output level remains at 17 dB SPL. The lowest (solid) PTC is predicted for no hearing loss, and the higher (dashed) ones are predicted for hearing losses of 20, 30, 40, and 50 dB. . . . .	41
4-11	Probe threshold and critical ratio at 1000 Hz as a function of noise spectrum level. The solid line is the probe threshold as a function of noise level, and the dashed line is the critical ratio, defined as the difference between the masked threshold and the noise spectrum level at that threshold. The masked threshold function is asymptotic to the probe's threshold in quiet (7 dB SPL) as the noise level decreases to inaudibility. The effects of the expansion simulator are shown on the right: with noise and probe input levels ( $L_N, L_P$ ), the output levels ( $L_N^*, L_P^*$ ) will still be on the masked threshold function, so the critical ratio will not change. . . . .	42
4-12	Iterative algorithm to predict the result of the critical ratio experiment. Tone frequency is set at 1 kHz. . . . .	43
4-13	Predicted masked thresholds in wide band noise as a function of noise level for a variety of simulated losses. . . . .	45
4-14	Effects of the bandpass nature of the expansion simulator in the simultaneous masking experiment. In Case 1, the probe tone (and auditory filter) is <i>centered</i> on one of the simulator's bandpass filters, which are depicted by alternating light and dark rectangles. In Case 2, the tone is placed at the very edge of one of the filters. As a result of the placement of the tone, different critical ratios may be measured. . . . .	46
5-1	Predictions and experimental data from the intensity discrimination experiment for subject JW; the three conditions are compared at equal sound pressure levels. Solid lines are the data from Rabinowitz et al. (bottom) and the expansion simulated prediction with a simulated flat 50 dB loss (top). Symbols are the data from the unsimulated case ( $\diamond$ ), expansion simulated case ( $\circ$ ), and noise simulated case ( $\triangle$ ). . . . .	51
5-2	These two panels contain the same data for JW as in Figure 5-1, but instead of comparing the three conditions at equal sound pressure levels, they are compared at equal <i>sensation levels</i> (left) and <i>equal loudness</i> (right). The legend is the same as in the previous figure. . . . .	51
5-3	Predictions and experimental data from the intensity discrimination experiment for subject KL. Legend is the same as in Figure 5-1. . . . .	52
5-4	These two panels contain the same data for KL as in Figure 5-3, but instead of comparing the three conditions at equal sound pressure levels, they are compared at equal <i>sensation levels</i> (left) and <i>equal loudness</i> (right). The legend is the same as in the previous figure. . . . .	52



5-5	Predictions and experimental data from the intensity discrimination experiment for subject JL. Legend is the same as in Figure 5-1. . . . .	53
5-6	These two panels contain the same data for JW as in Figure 5-3, but instead of comparing the three conditions at equal sound pressure levels, they are compared at equal <i>sensation levels</i> (left) and <i>equal loudness</i> (right). The legend is the same as in the previous figure. . . . .	53
5-7	Predictions and experimental data from the PTC experiment with subject DL. The solid lines are the <i>predicted</i> PTCs in the unsimulated condition (bottom) and with an expansion simulated flat loss of 40 dB (top). Symbols show the data from the unsimulated case ( $\diamond$ ), expansion simulated case ( $\circ$ ), and noise simulated case ( $\triangle$ ). The level and frequency of the probe in the unsimulated and simulated cases is given by the filled $\diamond$ symbols. . . . .	54
5-8	Predictions and experimental data from the PTC experiment with subject AM. The legend is the same as in Figure 5-7. . . . .	55
5-9	Predictions and experimental data from the simultaneous masking experiment for subject JW. Lines are the threshold-fitted Hawkins and Stevens data (solid) and the prediction of the results of an expansion-simulated 40 dB loss (dashed). Symbols show data from the unsimulated condition ( $\diamond$ ), expansion simulated condition ( $\circ$ ), and noise simulated condition ( $\triangle$ ). . . . .	56
5-10	Predictions and experimental data from the critical ratio experiments for subject KL. Legend is the same as for Figure 5-9. . . . .	56
5-11	Predictions and experimental data from the critical ratio experiments for subject JL. Legend is the same as for Figure 5-9. . . . .	57
5-12	Filterbank effects of changing the probe frequency in the expansion simulated condition for subject JW. Symbol size increases as the frequency increases from the extreme edge of the band (945 Hz) to nearer the center (955 Hz and 1000 Hz). . . . .	58
5-13	Filterbank effects of changing the probe frequency in the expansion simulated condition for subject KL. Symbol size increases as the frequency increases from the edge of the band (955 Hz) to nearer the center (1000 Hz). . . . .	58
5-14	Data from the unsimulated condition of the suppression experiments ( $\diamond$ ) shown with data from Shannon (solid line). Probe tone was at 1000 Hz. Each data point measures the amount of masking as a function of suppressor frequency, so that negative values indicate suppression. The threshold for the probe tone with no suppressor present (i.e. 0 dB of masking) was 30.7 dB SPL. . . . .	59
5-15	Identical to Figure 5-15, except that the probe tone was at 2000 Hz. The threshold for this probe with no suppressor present (i.e. 0 dB of masking) was 32.4 dB SPL. . . . .	59

A-1 Data from the intensity discrimination experiment for subject JW. Data points are shown for the unsimulated case ( $\diamond$ ), the expansion simulated case ( $\circ$ ), and the noise simulated case ( $\triangle$ ). Solid lines are the best-fit sigmoid through the data points. Overall sound levels are indicated at the top of each panel. . . . . 69

A-2 Data for subject KL. Legend is identical to Figure A-1. . . . . 70

A-3 Data for subject JL. Legend is identical to Figure A-1, except that fewer experimental conditions were examined. . . . . 71

A-4 Decision space for the 2AFC intensity discrimination experiment. . . . . 71

A-5 Conditional probability densities for the difference of the two observations  $X_1$  and  $X_2$ . 71

A-6 The two domains of the intensity discrimination experiment. In the “percent correct domain,” the function relating Bel intensity difference to percent correct is a sigmoid. In the “ $d'$  domain”, the function relating Bel intensity difference to  $d'$  is a straight line through the origin with slope  $\delta'$ . Translations are made between domains by means of Equation A.1. . . . . 72

# List of Tables

4.1	Size of the filterbank effect, in decibels, for simulated hearing losses between 20 and 50 dB and four noise levels. . . . .	48
6.1	Effect of the two hearing loss simulations and real impairment on intensity discrimination when compared with normal data at equal sound pressure levels, equal sensation levels, and equal loudness. A “+” indicates <i>better than normal</i> sensitivity, a “-” indicates <i>worse than normal</i> sensitivity, and the absence of a symbol means that the results were ambiguous. Impaired data was taken from Florentine et al.’s “flat audiograms.” . . . . .	61
7.1	Some existing sources to characterize the simulation of hearing loss. . . . .	65

# Chapter 1

## Introduction

This thesis is an outgrowth of the author's 1994 MIT Advanced Undergraduate Project [14]. The underlying purpose of the work has been to characterize the effects of a new kind of hearing loss simulation by performing psychoacoustic experiments with human subjects. The simulator is a signal processing system which simulates the effects of sensorineural hearing loss by means of amplitude expansion. It is hypothesized that when subjects with normal hearing listen to sounds which have been processed by the simulator, their performance will be similar to that of *real impaired* subjects listening to the *unprocessed* stimuli.

The next section provides background information relevant to hearing science, hearing impairment, and hearing loss simulations; the following section presents the goals of this thesis.

### 1.1 Background

Section 1.1.1 defines some of the psychoacoustics terms which are used in the rest of the thesis. Section 1.1.2 introduces several types of hearing impairments and describes their effects. Section 1.1.3 presents two methods of simulating hearing loss and reviews previous scientific studies of their effects.

#### 1.1.1 Psychoacoustics

Psychoacoustics is a section of hearing science which deals with the psychology of hearing. It is one branch of the broader science of psychophysics, which is defined as “the investigation of the relations between physical stimuli and psychic action in the production of sensations <sup>1</sup>.” Simply put, a psychoacoustician tries to find out how the sounds he or she can physically measure are perceived by the mind. Often the simplest sounds to work with are *pure tones*: these are sinusoidal

---

<sup>1</sup>This term was first used in *Rep. Brit. Assoc. Adv. Sci. 1877 ii. 95*: “Most of you are aware of the recent progress of what has been termed *Psycho-physics*, or the science of subjecting mental processes to physical measurements and to physical laws.”

signals which contain only one frequency. Another often-used sound is *white noise*, a random signal which has equal energy at all frequencies. White noise can be filtered, which is analogous to adjusting its treble and bass content. Filtered white noise is often called “shaped noise.”

One of the reasons that pure tones are so attractive to psychoacousticians is the fact that *any* other sound can be built up by adding together enough pure tones of different frequencies (this is called Fourier synthesis). Another appealing property of pure tones is that much *physiological* research has also been done using them as stimuli, and the ear’s neural response to a tone is well understood. [21, Chapter 3].

Another term which will be used in this paper is *masking*. Masking occurs when one sound interferes with the perception of another. The presence of the first sound can make the second sound harder to hear than when it is presented all by itself; the first tone is said to *mask* the second one. [21, p. 104]. Masking is quite intuitive; think about trying to listen to one person talking in a crowd of people. *Simultaneous masking* occurs when two sounds are present simultaneously; other kinds of masking can occur when they are not. A first sound which is *not* present at the same time as a second sound can still mask the second one as long as the time between their presentations is short. [21, p. 261]. This phenomenon is called *forward masking*.

The term *threshold* refers to the quietest sound that a person can distinguish from silence; if the form of the sound is not specified then it is assumed to be a pure tone. *Masked threshold* is the quietest signal that a person can distinguish from no signal in the presence of a masking sound. *Discrimination* is a person’s ability to perceive the difference between two sounds which differ by a small amount in intensity, frequency, etc. *Frequency selectivity* describes how well a person can focus on detecting a signal at one frequency while rejecting signals at other frequencies.

### 1.1.2 Hearing Loss

The three kinds of hearing loss are conductive, sensorineural, and central. They may occur individually, in which case they are called “pure losses,” or in combinations. A *conductive* hearing loss arises from abnormal functioning of the structures which carry sound vibrations from the air to the fluid-filled inner ear. *Sensorineural* loss is a result of abnormal functioning of the inner ear cells which transduce sound energy into electrical currents or of the auditory nerve fibers which carry neural signals produced by those cells. *Central* hearing loss cannot be explained by a malfunctioning of the ear; it involves abnormalities in the higher auditory centers of the brain. Central hearing loss may cause an impairment in speech perception but not in pure tone reception; it is quite a different problem than the other kinds, and no further mention of it will be made.

The most common kind of hearing loss is *sensorineural hearing loss of cochlear origin* [21, p. 297]. It is the result of damage to the inner and outer hair cells of the cochlea (inner ear), and it can result from old age, acoustic overstimulation, drugs, and infections; it can also be a congenital condition.

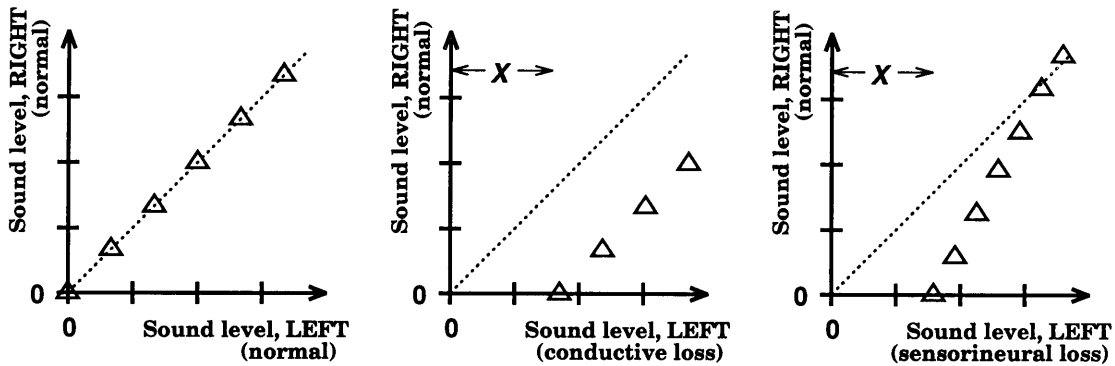


Figure 1-1: Schematized results of a loudness balancing experiment with a normal subject (left), a subject with a monaural pure conductive loss (middle), and a subject with a monaural pure sensorineural loss. (right). The “ $\Delta$ ” symbols indicate points of equal loudness. Roughly speaking, the degree of hearing loss is given by the difference  $X$ .

Sensorineural loss is more serious than conductive loss, because it introduces distortions which are not equivalent to linear filtering [26, p.240] and therefore cannot be corrected by inverse filtering alone. A good way to contrast the effects of conductive and sensorineural loss is by performing a loudness balancing experiment.

### Loudness Balancing

In a loudness balancing experiment, a subject is presented with pure tones alternately in both ears; he is then asked to adjust the level of the tone in one ear until it sounds “equally loud” as the fixed-level tone in his other ear. Each resulting pair of physical sound levels, (**left ear level, right ear level**) is used to plot an (x,y) point on a graph. Figure 1-1 presents schematized results for a subject with two normally functioning ears (left); one normal ear and one ear with conductive loss (center); and one normal ear and one ear with sensorineural loss (right).

In the case of the normal-hearing subject, the points of equal loudness fall on the line with unity slope which passes through the origin; in other words, two normal ears perceive equal loudness at equal physical sound levels.

In the case of the pure conductive loss, the line describing the points of equal loudness has been shifted to the right by a fixed amount. All tones in the impaired ear sound  $X$  dB quieter than they do in the normal ear, no matter what the level. Conductive hearing loss is equivalent to linear filtering (frequency-dependent attenuation) and can be completely corrected by filtering with the inverse system (amplification).

In the case of the pure sensorineural loss, points of equal loudness no longer lie on a line with unity slope. The difference between perceived loudness in the normal and impaired ears is a function of *level*. At low sound levels, the results are similar to the results of a conductive loss: tones in the

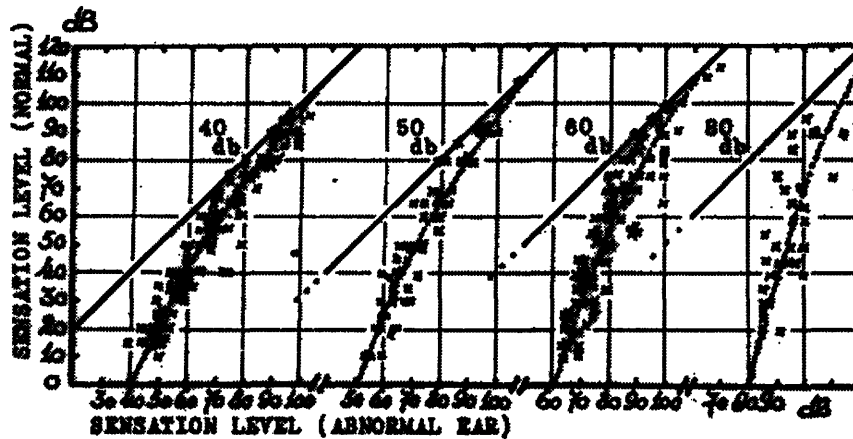


Figure 1-2: Recruitment in monaurally impaired subjects. At conditions of equal loudness, the  $x$ 's plot intensity of tones in the normal ears (vertical axis) versus intensity of tones in the impaired ears (horizontal axis). This figure is from Miskolczy-Fodor, 1960.

impaired ear sound  $X$  dB quieter than they do in the normal ear. However, at high sound levels the effects of the hearing loss are lessened. At a sufficiently high level (called the “threshold of complete recruitment”) both ears perceive equal loudness at equal physical levels, matching the results from the case of *no* hearing loss. This phenomenon, associated only with sensorineural hearing loss, is called *recruitment*. Because the points of equal loudness do not lie on a line with unity slope, recruiting hearing loss cannot be corrected by linear filtering. Using enough amplification to make weak sounds audible would render strong sounds unpleasantly loud.

Figure 1-2 shows experimental data from a loudness balancing experiment by Miskolczy-Fodor [16]. The subjects all had monaural sensorineural losses, and they were grouped into four broad categories depending on their degree of loss: 40, 50, 60, and 80 dB. This figure shows that as hearing loss increases, so does the slope of the line of equal loudness. It can also be used to describe why recruitment is described as “abnormally rapid growth of loudness with increasing level.” For a normal ear (vertical axis), loudness grows from inaudibility to discomfort over a span of about 100 decibels. For the impaired ears, loudness covers the same subjective range over a much smaller physical dynamic range: about 60 dB in the case of a 40 dB loss. Therefore, for a given increase in level, loudness increases more for an impaired person than for a normal hearing person.

In the rest of the thesis, the term “hearing loss” will be used as shorthand for “sensorineural hearing loss.” Conductive loss will not be mentioned again.

### 1.1.3 Hearing Loss Simulation

This section describes two methods of simulating sensorineural hearing loss: additive noise and amplitude expansion. Both methods can simulate reduced sensitivity to weak sounds and recruitment,

and both methods are investigated in the experiments of this thesis.

### **Additive Noise**

The addition of broadband white noise to a signal is one way to simulate hearing loss. Hawkins and Stevens [12] have shown that pure tone detection thresholds in broadband noise increase as an orderly function of increasing noise power. For example, to raise a person's 1 kHz threshold to 50 dB SPL, the person should be exposed to noise with a power of 30 dB/Hz at 1 kHz. An arbitrary set of frequency-dependent thresholds can be simulated by shaping white noise to have proper amounts of energy at each frequency. This process is called "equivalent threshold masking" (ETM).

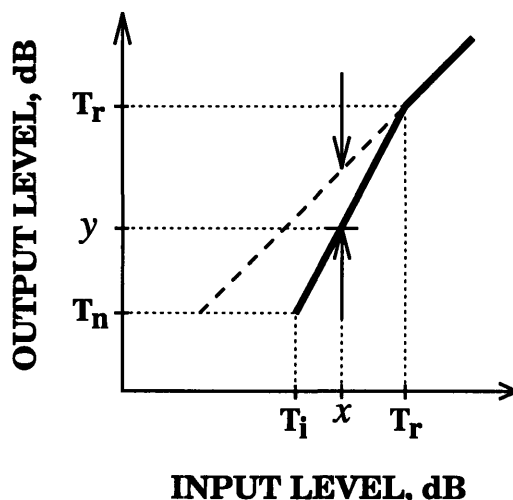
Like real hearing impairments, ETM also causes recruitment when used with normal-hearing subjects. Adding random noise to a signal raises its detection threshold but does not raise the threshold of discomfort. The result is abnormal loudness growth (recruitment).

One disadvantage of using additive noise is that simulations must be limited to mild to moderate losses of less than 60-70 dB [5]. The noise levels necessary to simulate more severe losses are unacceptable for prolonged exposure. There is also a perceptual problem with noise simulations: people with real impairments don't necessarily experience a constant noise.

Many studies of hearing impaired subjects have been performed using equivalent threshold masked normal subjects to control for the effects of elevated thresholds and high stimulus levels. The studies have used both traditional psychoacoustic stimuli and speech stimuli. For example, Zurek and Delhorne [29] examined consonant reception in impaired subjects and noise-masked normal subjects. They discovered similar results in both populations, suggesting that additive noise is a good simulation for this experiment. Dubno and Schaefer [4] made several different measurements of the frequency selectivity of both impaired subjects and noise masked normal subjects. Using forward masked tuning curves, they found that frequency selectivity is worse than normal for both populations, but that the noise masked subjects still outperformed the impaired subjects. Dubno and Schaefer also measured the critical ratios of both impaired subjects and noise masked normal subjects and found essentially no correlation between impaired threshold and critical ratio [4]. Florentine et al. [9] studied intensity discrimination in impaired and noise masked subjects. In general, they found that the impaired population displayed worse than normal sensitivity when compared at equal sound levels or equal loudness and normal (or better) sensitivity when compared at equal sensation levels. Like Dubno and Schaefer, they found that the performance of the noise masked normal subjects was comparable to the impaired results but that not all of the detrimental effects of hearing loss were captured by the simulation.



Figure 1-3: Loudness balancing curve reinterpreted as a simulator input/output function. The solid line is the input/output function, with a reference gain of unity indicated by the dashed line. Normal threshold is marked  $T_n$ , impaired threshold as  $T_i$ , and the threshold of complete recruitment as  $T_r$ .



### Level Expansion

A different way to produce the elevated thresholds and recruitment of hearing loss is to use signal processing which applies a level-dependent attenuation, as shown in Figure 1-3. The bold line in the figure is an idealization of the impaired loudness balancing curves shown in Figure 1-2, with the dashed line representing the equal loudness contour of a normal listener. The abscissa may be reinterpreted as the input of a hearing loss simulator with the output as the ordinate. For example, according to the loudness balancing curve, the sound level  $x$  is equally loud in an impaired ear to the sound level  $y$  in a normal ear. To present an input signal at  $x$  to a normal listener at the same loudness as for the impaired listener, it must be attenuated by the amount indicated by the arrows so that the output level is  $y$ .

Expansion simulators apply a level-dependent, frequency-dependent attenuation. The need for level dependence is clear: above the threshold of complete recruitment no attenuation need be applied; below the impaired threshold infinite attenuation can be applied because the signal becomes inaudible. The frequency dependence of the attenuation arises because the slope and boundaries of the loudness balance curve in Figure 1-2 (and hence the input/output function in Figure 1-3) may change with frequency, depending on the hearing loss. One way to achieve frequency dependency is to band pass filter the input into separate frequency ranges and process each band independently. This kind of system is called an *expansion simulation* because output level changes are greater than input level changes. Because the slope of the input/output function is greater than one for inputs between  $T_i$  and  $T_r$ , a fluctuation in input level of 1 dB will correspond to an expanded fluctuation

at the output of  $K$  ( $> 1$ ) dB, where  $K$  is the slope of the input/output curve.

Because expansion simulations work by attenuating the input rather than adding masking noise, they can be used to simulate more severe impairments. Additionally, they do not require the constant presentation of a masking signal and may therefore be more perceptually accurate than noise simulations [28].

Less extensive study has been made of expansion simulations than of noise simulations, mainly because they require more hardware and/or processing power to implement. A qualitative test was made of an analog 4-channel simulation by Villchur [28] in which monaurally impaired subjects were asked to judge the similarity of the simulation and their real impairment. The responses were all “very similar” or “similar.” Duchnowski [5] implemented a 14-channel simulation in software and performed speech intelligibility experiments using both consonant vowel pairs and sentence material. His results showed good agreement between his impaired subjects and simulated normals, in terms of both percent correct scores and error patterns. For an Advanced Undergraduate Project at MIT, Lum also investigated Duchnowski’s 14-channel simulation, this time implementing it as a real-time system [14]. He evaluated the system’s effects on simple input signals such as tone bursts and also performed psychoacoustic experiments including measuring forward masked tuning curves and narrow band noise masking patterns.

## 1.2 Goals

The fundamental goal of this project was to gather and interpret data describing the performance of normal hearing subjects using the Duchnowski/Lum expansion simulation. Since there is already much data from experiments in speech reception [5], the experiments in this thesis involved more traditional psychoacoustic stimuli: tones and noise. The particular experiments that were performed included: measuring intensity discrimination; measuring the simultaneous masking induced by broadband noise; and measuring two tone suppression. To account for subject variability, all experiments were first performed using no simulation of hearing loss (referred to as the “unsimulated condition.” The same experiments were then performed using the Duchnowski/Lum simulation (the “expansion simulated condition”) and also using equivalent threshold noise masking (the “noise simulated condition”). In Chapter 6 data from the two simulated conditions are compared with each other and with existing data from impaired subjects.

To achieve the stated goal, the work of the thesis was conceptually divided into three phases: software development, modelling and prediction, and experimentation. The software development work was intended to augment the capabilities of the software tools invented by the author as part of his AUP. The modelling and prediction was done to promote a better understanding of the data from the expansion simulated condition. For each experiment, the expansion simulated

results were *predicted* by forming a model of the system, determining what the output would be, and using existing psychophysical data to predict how a normal hearing subject would respond to that output. Predictions were made not only of the experiments performed in this thesis, but also of an experiment done in the author's AUP: forward masked tuning curve measurement. Chapter 2 describes the software development work. Chapter 3 describes the experiments in this thesis as well as the tuning curve experiment from the AUP. Chapter 4 describes how the modelling and prediction was done for each experiment. Chapter 5 presents the experimental data, and Chapter 6 discusses it.

## Chapter 2

# Software Development

The software written for this project falls into two categories, each of which is meant to solve a separate problem. The first category is *low-level software*, written at the assembly-code level; it removes an unnecessary analog communication channel from the experimental setup used in the author's AUP. The second category is *high-level software*, written in *C* and *Espud*, a *LISP*-like language; this software provides a user interface for the design and execution of computer-controlled psychoacoustic experiments. The low-level and high-level software is treated in Sections 2.2 and 2.3, respectively.

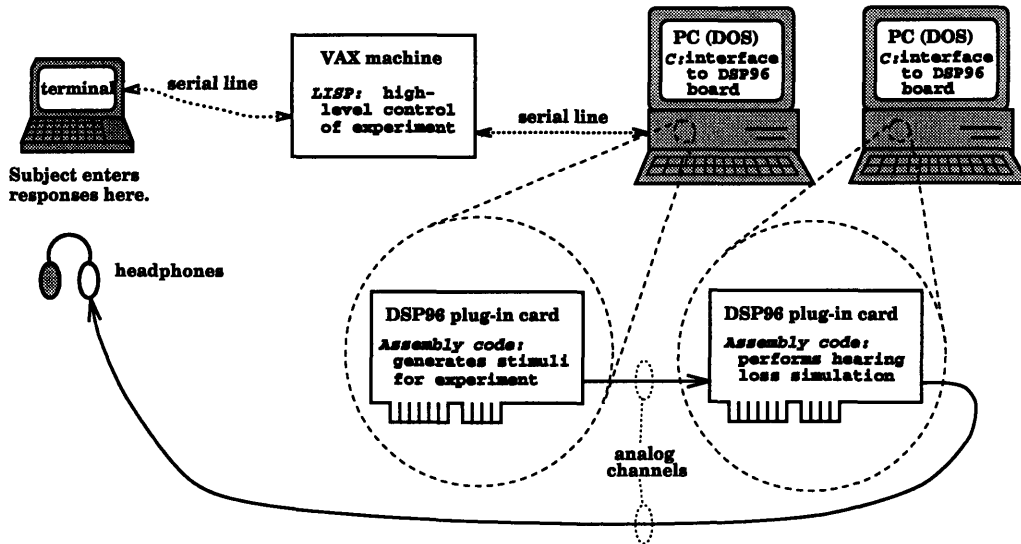
### 2.1 Laboratory Setup

The detailed description of the thesis software in the following sections becomes much more understandable with the help of a description of the laboratory setup during a psychoacoustic experiment. Figure 2-1 shows the computers and apparatus in use during an experiment, as well as the interconnections between machines. Note that this is the original setup which was used in the author's AUP; the improvements made on it during this thesis are the topic of this chapter.

The centerpiece of any psychoacoustic experiment is the human subject who is listening to stimuli, making judgements, and reporting what he or she has heard. In our setup, the subject sat in front of a computer terminal inside a double-walled soundproof booth, wearing headphones. The position of the subject in Figure 2-1 is in the upper left corner. Sound stimulus was delivered through the headphones, and the subject entered responses into the computer terminal to be recorded.

The response terminal was connected via a serial line to a VAX computer, which ran the high-level experiment control language described in Section 2.3. To make changes in the sound stimuli, the VAX machine sent commands to the DSP board which actually generated them. These commands also traveled over a serial line to the DSP board's host PC (IBM-compatible microcomputer), which interpreted them and sent them to the DSP board contained within it.

Figure 2-1: Original laboratory setup for psychoacoustics experiments in the author's AUP. Note the noisy analog channel between DSP boards.



Before the sounds generated by the DSP board in the center of Figure 2-1 reached the subject's headphones, they were processed to effect the simulation of hearing loss. The digital stimuli were converted to an analog signal and sent through an analog channel to *another* DSP board, which performed the hearing loss simulation and sent the resulting signal to the subject's headphones.

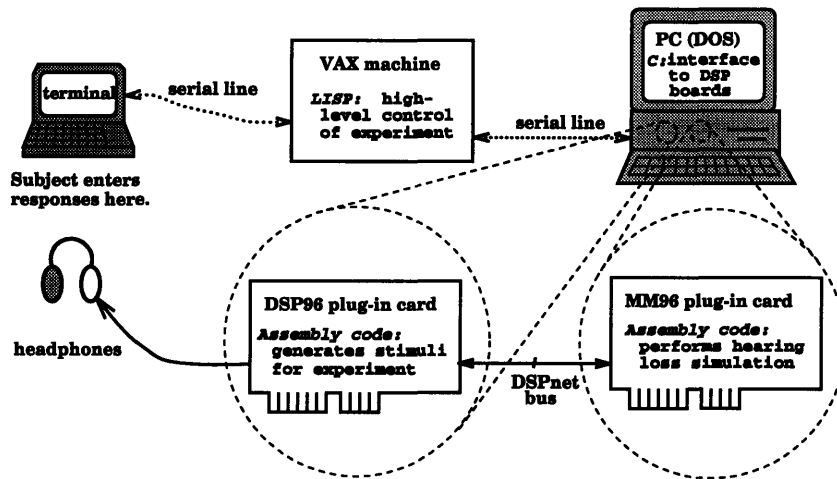
## 2.2 Low-level Software

### 2.2.1 Purpose

The purpose of the low-level software improvements was to eliminate the analog channel connecting the two DSP boards in Figure 2-1 and replace it with a digital channel, as shown in Figure 2-2. The benefit of this substitution is twofold.

The first advantage is an increase in the signal-to-noise ratio of all stimuli, which is especially important at low levels. Since the analog channel always has the possibility of picking up spurious noise signals, the stimuli sent through it must be kept at a high level to maintain a good signal-to-noise ratio. So, if the experimenter wishes to use good-quality low-level stimuli in his or her experiments, he or she must generate stimuli at an artificially high level for transmission across the analog channel and then compensate for the amplification by applying a complementary attenuation at a later stage. A further difficulty arises at the hearing loss simulator; because the simulator does its processing in a *level-dependent* way, it must somehow be informed that the experimenter has

Figure 2-2: New laboratory setup, improved due to much new software and some new hardware.



artificially raised the level of its input. Using a digital channel between DSP boards eliminates these problems.

The second advantage is that the dynamic range at the input to the hearing loss simulator is vastly increased. The original lab setup in Figure 2-1 used an analog channel to connect two DSP boards, which meant that the original 32 bit floating-point signal generated by the first DSP board was converted to a 16 bit integer, quantized to an analog signal, and then sent to the second DSP board for hearing loss simulation. The use of a channel involving 16 bit integers dictated that the dynamic range of any signal could only be 90 dB *at most*. When a 32 bit digital communication channel is used as in Figure 2-2, 32 bit floating point values may be transmitted between boards, which allows the signal to have a vastly greater dynamic range.

An additional change in the equipment is also visible from a comparison of Figures 2-1 and 2-2. To reduce the number of laboratory PCs used in the experiments, two DSP cards were installed in a single PC.

### 2.2.2 Implementation

The 32 bit channel between DSP boards was implemented using *DSPnet*, a multi-master, parallel expansion bus for interconnecting devices made by the Ariel company [2]. Physically, *DSPnet* is a 50-pin ribbon cable connecting two DSP boards in a single PC. The software to control the bus was written in assembly code.

## 2.3 High-level Software

### 2.3.1 Purpose

The purpose of the high-level software was to provide a user interface for designing and controlling psychoacoustic experiments involving tone and noise stimuli. The interface was built on top of *Espud*<sup>1</sup>, a *LISP*-like interpreter which was already capable of controlling much laboratory apparatus via serial lines. With the additional software written for this thesis, *Espud* gained the capability of controlling tone and noise generators on lab Ariel DSP boards.

### 2.3.2 Implementation

Implementing the enhancements to *Espud* required writing *Spud* routines to communicate with the PCs which contain DSP boards. *C* code was also written to allow the PCs to interpret the commands sent by *Espud* and download the proper data and commands to the DSP boards contained within.

## 2.4 Documentation

A user's guide was written which explains the use of both the *Espud* functions and the *C* programs running on the PC [15].

---

<sup>1</sup>*Espud* is itself based on Peterson and Frisbie's *Spud* signal processing environment [20].

## Chapter 3

# Experiments

This chapter introduces each psychophysical experiment and explains why it was chosen to characterize the expansion simulator. For each section here, there is a corresponding section in Chapter 4 which models the expansion simulator and predicts the experimental results. There is also a corresponding section in Chapter 5 which presents the experimental data.

Five subjects were used, although each did not participate in all of the experiments. The subjects (DL, JL, KL, AM, and JW) were all college students in their early '20s with clinically normal<sup>1</sup> hearing. They were paid for their participation. All experiments were performed with the subject seated before a computer terminal inside a soundproof booth. Stimuli were generated digitally with 16 bit precision and presented to the subject through a set of Telephonics TDH-39P (296D000-2, serial #072681) headphones whose frequency response was measured to be fairly flat from 50 Hz to 4 kHz [14, p.30].

### 3.1 Intensity Discrimination

Intensity discrimination refers to a subject's ability to discern a difference between two sounds of different intensities. It is an interesting psychoacoustic ability to measure in conjunction with the expansion simulator precisely due to the simulator's "expanding" input/output characteristic. As shown in Figure 1-3, the static transfer function of the simulator has a slope greater than unity in the recruiting region. In this region, slow fluctuations of 1 decibel at the input will be heard at the output as fluctuations of greater than 1 dB, and intensity discrimination will presumably improve.

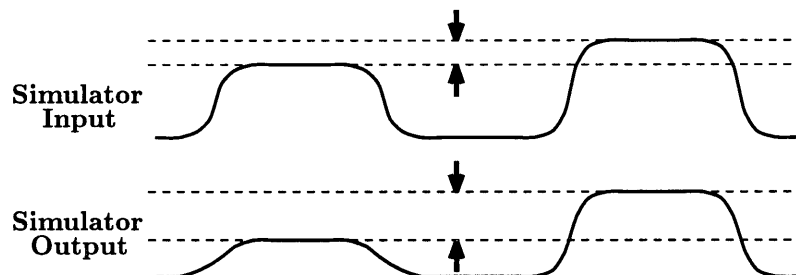
Figure 3-1 illustrates the expansion effect graphically. At the input to the simulator are two tone bursts, differing in intensity by a small amount. At the output, the intensity difference has been *magnified* by a factor which depends on the severity of the simulated hearing loss. A subject who

---

<sup>1</sup>Pure tone thresholds were less than 20 dB HL [1] for frequencies between 250 and 4000 Hz.



Figure 3-1: Effects of the expansion simulator on the intensity discrimination stimuli. At the input, tone bursts are separated by a small intensity difference. At the output, the difference in intensity is exaggerated and the overall level has been reduced.



could not detect the small intensity difference at the input to the system may be able to hear it at the output due to the expansion. Thus, it seems that the expansion simulator should actually improve a subject's intensity discrimination.

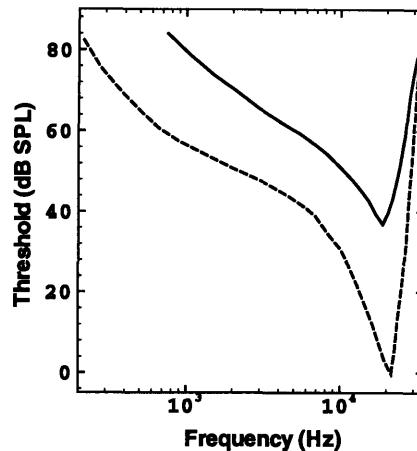
The situation is somewhat more complicated, however. In addition to the level-expansion effect, Figure 3-1 also shows the other major effect of the simulator: the tone bursts at the output have been *attenuated* relative to the input. Attenuation of the signal has been shown to reduce intensity discrimination [22], which suggests that a subject may not experience as large an improvement in intensity discrimination as predicted based solely on the amount of expansion. The two main effects of the expansion simulator, level expansion and overall attenuation, have opposing effects on intensity discrimination, and a more quantitative examination is required to determine which effect dominates. The expansion simulation would be considered more accurate if it were shown *not* to increase intensity discrimination beyond the normal range, because research on real impaired subjects shows either no change or a decrease in this ability relative to unimpaired subjects [9].

### 3.1.1 Experimental Parameters

The sound stimuli were of the form of Figure 3-1. Two tone bursts were presented, differing in intensity by a fixed amount which remained constant over a set of 40 presentations (a "fixed level paradigm"). The sequences (**loud, soft**) and (**soft, loud**) had an equal probability of occurring on each presentation, and the subject was asked to identify the louder tone burst in each trial. The number of correct responses was divided by the total number of presentations to determine a percent correct score. After each set of 40 trials the intensity difference was changed, and the function relating percent correct to decibel difference was used to calculate intensity discrimination in sensitivity-per-Bel, as described in Appendix A.

The tone burst on times were 400 ms, and the interburst silence was 250 ms in duration. Rise and

Figure 3-2: Comparison of a neural tuning curve from an undamaged cochlea (dashed line) with an NTC from a cochlea whose inner and outer hair cells had both been damaged (solid line). Liberman and Dodds, 1984.



fall times were identically 25 ms, and the shape of the transients was cosinusoidal. The frequency of the tones was 1000 Hz. Several overall presentation levels were used: 40, 70, 80, and 85 dB SPL in the unsimulated condition and 70, 80, and 85 dB SPL in both simulated conditions.

## 3.2 Psychophysical Tuning Curves

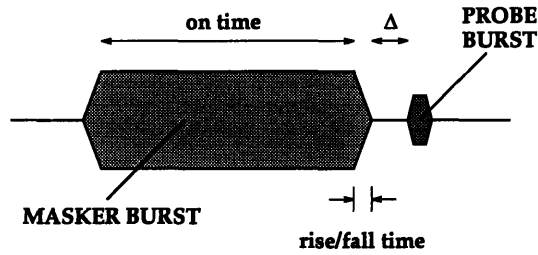
Although this experiment was performed in the author's AUP, it is discussed again here in preparation for the chapter on predictions. As a way of introducing the subject of psychophysical tuning curves (PTCs), the more straightforward neural tuning curve (NTC) will be discussed. Both PTCs and NTCs measure the ear's frequency selectivity, which is generally worse than normal in subjects with hearing loss [4]. To be an accurate simulation of hearing loss, the expansion simulator should reduce the frequency selectivity of normal hearing subjects.

### 3.2.1 Neural Tuning Curves

One way to study the effects of sensorineural hearing loss is to make direct measurements of the neural signals produced by the damaged transducer cells of the inner ear. Experiments of this type have shown that damage to the inner and outer hair cells of the cochlea causes a substantial change in the shape of the function which relates pure tone "neural threshold"<sup>2</sup> to frequency [13]. Figure 3-2, from Liberman and Dodds [13], compares two such neural tuning curves measured from the auditory

<sup>2</sup>Neural threshold is defined as the sound level which results in an increase in an auditory nerve fiber's neural discharge rate by a specified percentage above its spontaneous rate.

Figure 3-3: A schematic of the stimulus in a forward-masked PTC experiment. A short, quiet probe tone is presented shortly after a longer, more intense masker tone.



nerve of a cat. The lower NTC is typical for a nerve fiber in an undamaged cochlea, and the upper one is typical for a fiber from a cochlea whose inner and outer hair cells have sustained damage due to noise overexposure.

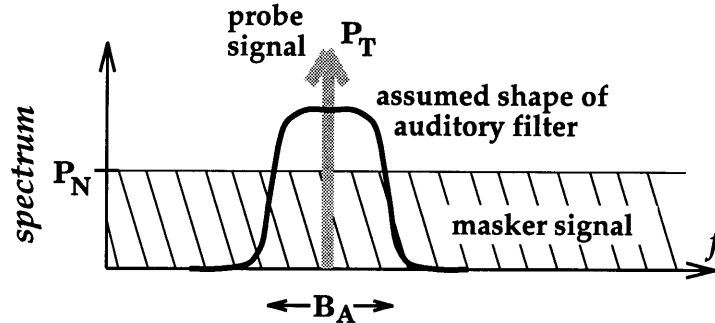
The effect of hearing loss is more pronounced at the center frequency of the nerve fiber ( $\sim 20$  kHz), where the vertical elevation between the normal and impaired tuning curves is almost 40 dB. At other frequencies, the effect is less severe. The result of this nonuniform elevation is that the NTC becomes less sharp near the tip and broader overall. Since there is such a dramatic difference between the normal and impaired NTCs, they would be an interesting thing to measure during hearing loss simulation. However, in practice it is impossible to make physiological measurements from a human subject’s auditory nerve; a psychophysicist has to rely on the next best thing, which is described in the following section.

### 3.2.2 Psychophysical Tuning Curves

*Neural* tuning curves describe, as a function of frequency, the tone intensity required to produce a specified increase in neural activity in a particular nerve fiber. *Psychophysical* tuning curves describe, as a function of frequency, the tone intensity required to mask a “probe tone” very near threshold at a fixed probe frequency. Since the probe tone is close to threshold, it is reasoned that only a small number of nerve fibers are able to respond to it, thus approximating the physiologist’s single-fiber experiment [21, p. 260].

Empirically speaking, neural and psychophysical tuning curves have proven to be very similar and are considered correlates of each other. Researchers have also found that the shape of the PTC is a closer match to the NTC when the masker tone and probe tone are presented *sequentially* rather than simultaneously [21, p. 268]. These “forward-masked PTCs” are the kind of tuning curves that were measured in the author’s AUP.

Figure 3-4: Use of a broadband masker and a narrow band probe to measure the bandwidth of an auditory filter.



### 3.2.3 Experimental Parameters

Figure 3-3 shows the stimuli used in the PTC experiment. A masker tone burst with a 200 ms on time precedes a probe tone burst with a 16 ms on time. The silent interval  $\Delta$  between bursts was 2 ms, and the cosinusoidal rise and fall times of all bursts were 7 ms.

The frequency of the probe tone was fixed at 1200 Hz. Its level was fixed at 20 dB above the subject's absolute threshold<sup>3</sup>. The masker frequency was varied between 600 and 1400 Hz, and at each frequency the threshold of masking was determined. To determine this threshold, a two-alternative forced-choice (2AFC) paradigm was used in which the stimulus in Figure 3-3 was presented twice with the probe tone randomly absent from one of the presentations. The subject was asked to indicate which presentation had contained the probe, and the threshold was determined by adaptively changing the masker level using the PEST [27] method with deviation limit  $W=1.0$  and target correct percentage  $P_t=0.75$ . The pause between the two presentations was 300 ms.

## 3.3 Simultaneous Masking

One way to measure the ear's frequency selectivity is to measure frequency tuning curves as described in Section 3.2. Another common method is to measure the masked threshold of a narrow band probe signal in the presence of a simultaneous broadband noise masker which can be low pass [18], bandpass [10], band stop [19], or all pass [8]. The bandwidth or shape of the ear's so-called "auditory filter" may be calculated from the masked threshold measurements, with the more complicated noise maskers tending to give measurements with better resolution [18, 19].

The basic idea behind using a broadband noise masker to measure frequency selectivity is illus-

trated in Figure 3-4. In the figure, white noise with power  $P_N$  in a one-Hertz band is used to mask a narrow band probe signal (pure tone) with power  $P_T$ . The subject is presumed to use an auditory filter centered on the probe to detect it, and the experimenter's goal is to calculate the shape or bandwidth  $B_A$  of this filter. If one is willing to approximate the filter shape as an ideal bandpass filter, then calculating its bandwidth requires only two pieces of information: the masked threshold and the signal-to-noise ratio  $S$  required for the probe to be detected.

Using the ideal bandpass approximation to the auditory filter, the signal-to-noise ratio  $S$  at threshold is

$$S = \frac{P_T}{P_N B_A} \quad (3.1)$$

Solving Equation 3.1 for the auditory filter bandwidth produces

$$B_A = \frac{P_T}{P_N S} \quad (3.2)$$

The important result of Equation 3.2 is that no matter what value of  $S$  is assumed, auditory filter bandwidth increases as the masked threshold  $P_T$  increases for fixed  $P_N$ .

This method of estimating auditory filter bandwidth was proposed by Fletcher, who chose to set the value of  $S$  to be 1.0 [8]. With this  $S$ , Equation 3.2 reduces to

$$B_A = \frac{P_T}{P_N} \quad (3.3)$$

Fletcher called the bandwidth, expressed in the form of Equation 3.3, the *critical ratio*. For a fixed noise spectrum level, a higher critical ratio suggests wider auditory filters, and thus poorer frequency selectivity. Calculating the critical ratio in dB from a masked threshold experiment is trivial: it requires subtracting the noise spectrum level in dB SPL/Hz ( $10 \log_{10} P_N$ ) from the tone level in dB at masked threshold ( $10 \log_{10} P_T$ ).

Despite the relationship between frequency selectivity and critical ratio in Equation 3.3, many persons with hearing loss do not exhibit higher than normal critical ratios at the same noise level. Dubno and Schaefer showed that there was essentially no correlation between critical ratio and absolute threshold for impaired subjects [4, p. 552]. The critical ratio seems to be too coarse a measure of frequency selectivity to capture the effects of sensorineural hearing loss. Nevertheless, it is still useful to see if the expansion simulator has any effect on it. The experimental results will be shown as masked thresholds ( $10 \log_{10} P_T$ ), but these can easily be converted to critical ratios by subtracting off the noise spectrum level.

---

<sup>3</sup>This level was chosen to be approximately 10 dB above the threshold of the 20 ms probe, which itself is approximately 10 dB above absolute threshold for a long duration tone[24].

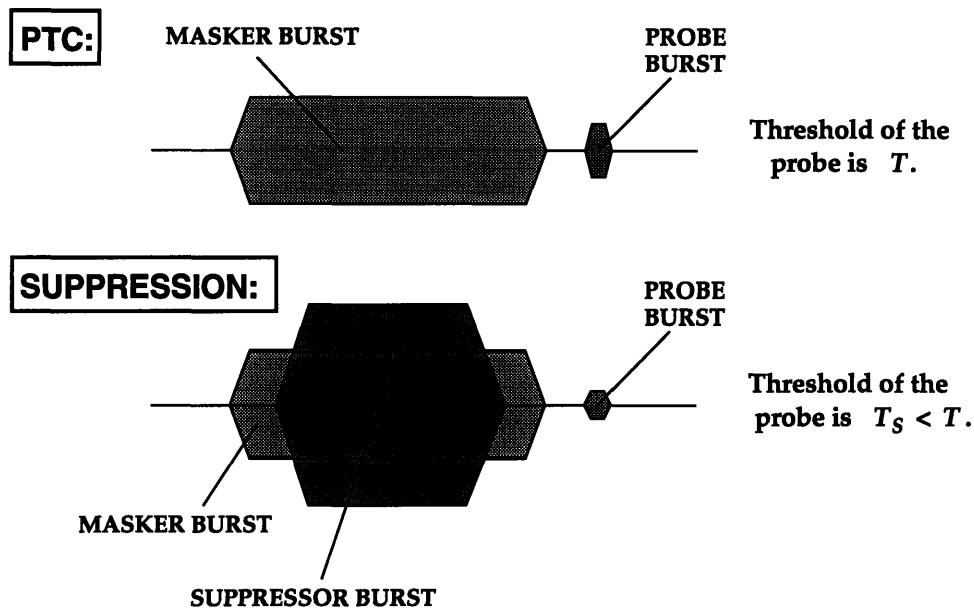


Figure 3-5: Comparison of the stimulus used in the PTC experiment with the stimulus used in the suppression experiment. In the suppression experiment, the masker intensity is fixed and the probe threshold  $T$  is measured. Adding a suppressor tone to the masker can actually *lower* the threshold of the probe to  $T_S$ .

### 3.3.1 Experimental Parameters

The stimuli were of the form of Figure 3-4. The narrow band probe signal was a pure tone at 1 kHz, and the broadband masker was white noise low pass filtered to 5 kHz. The noise power was varied between 20 dB/Hz and 60 dB/Hz, and the probe threshold was determined for each noise level. To determine the probe threshold, a 2AFC paradigm was used in which two sequential bursts of noise were presented with a randomly-selected one containing a simultaneous probe tone. The subject was asked which noise burst had contained the tone, and his 75% correct level was found adaptively using the PEST procedure. The rise and fall times of the noise and noise+tone bursts were 20 ms and cosinusoidal. On times were 400 ms, and the interburst-burst time was 300 ms.

## 3.4 Two Tone Suppression

A healthy inner ear exhibits a variety of nonlinearities, one of which is seen in the phenomenon of two tone suppression. An auditory nerve fiber may respond *less* strongly to a pair of simultaneous tones than it does to *one* of the tones presented individually. One tone is said to “suppress” the response caused by the other. [21, p. 99]. Suppression can’t occur in a linear system with two uncorrelated inputs. By definition, the response of a linear system to two inputs must be the sum

of its responses to each individual input; if the inputs are uncorrelated, then the outputs will also be uncorrelated, and the sum will contain more power than either individual output.

Psychoacousticians measure suppression by using a variation on the psychophysical tuning curve experiment described in Section 3.2 [23], [7, p.296]. Figure 3-5 shows the difference between the stimulus used in the PTC experiment and the stimulus used in the suppression experiment.

In the PTC experiment, the goal is to find out how intense a masker tone must be to obliterate the effects of a fixed-level probe tone. In the suppression experiment, the level of the masker is fixed, and the masked threshold of the probe,  $T$ , is measured (top of Figure 3-5). To produce suppression, a second suppressor tone is presented simultaneously with the masker. If the frequencies and durations of the tones are chosen properly, the masker can be suppressed, resulting in less masking and a lower masked probe threshold  $T_S$  (bottom of Figure 3-5).

Two tone suppression is an interesting phenomenon to study in conjunction with hearing loss simulation because it is typically absent in persons with sensorineural hearing loss [7, p.296]. The goal of this experiment is to determine whether the simulations preserve or destroy suppression.

### 3.4.1 Experimental Parameters

Following Shannon [23], both the probe and masker tones were fixed at a frequency,  $f_p$ . In the experiments,  $f_p$  was either 1000 Hz or 2000 Hz. The level of the masker was fixed at 40 dB SPL. A base line masked probe threshold was measured in the absence of any suppressor tone, and all subsequent measurements of “suppression” make implicit reference to this base line value. For example, if the masked probe threshold in the presence of a particular suppressor tone is 2 dB below the base line, the suppressor is said to cause 2 dB of suppression. The suppressor level was fixed at 60 dB SPL, and its frequency  $f_v$  was varied. For  $f_p = 1000$  Hz,  $f_v$  was varied between 900 and 1300 Hz; for  $f_p = 2000$  Hz,  $f_v$  was varied between 2300 and 2500 Hz. Based on the findings of Shannon [23] and Wightman [7, p.296], suppression was expected in these frequency ranges.

The suppressor and masker tones were present simultaneously and gated on and off at the same times (unlike Figure 3-5) with 20 ms cosinusoidal rise and fall times. The suppressor/masker combination had an on time of 500 ms, and the interval of silence between it and the probe was 0 ms. The probe tone had a 10 ms cosinusoidal rise and fall time with *no* on time (for a total length of 20 ms). The timing parameters of the experiment were also based on the experiments of Shannon.

To determine the masked probe threshold, an adaptive 2AFC experiment was performed to find the 75% correct level, the same as in the psychoacoustic tuning curve experiment.

## Chapter 4

# Modelling and Predictions

In this section, a method for predicting the outcome of the expansion simulated experiments will be presented. The method requires only two pieces of prior information: a model of the expansion simulator's input/output characteristic and a detailed description of the function which relates the experiment's dependent variable to the independent ones for a normal hearing listener. The first piece of information can be obtained from an understanding of the input/output behavior of the simulator. The second piece is drawn from the vast psychoacoustics literature characterizing normal hearing ears.

Each of the following sections analyzes a single psychoacoustic experiment from Chapter 3. The experiment is described, the data in the literature for normal hearing subjects is discussed, and the results of the expansion-simulated condition are predicted.

### 4.1 Intensity Discrimination

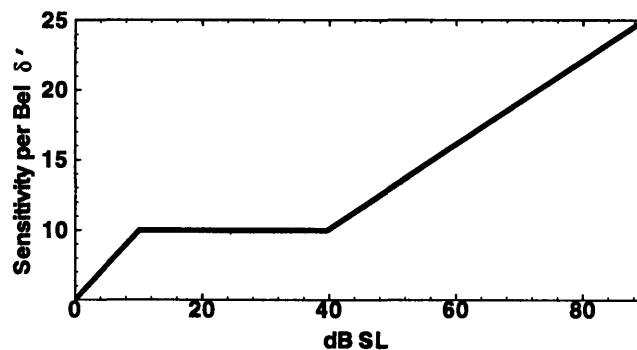
For the prediction of the intensity discrimination experiment, the stimulus tone bursts from Figure 3-1 will be treated as if they were infinite-duration sinusoids so that the simulator's static input/output function of Figure 1-3 may be used. In a previous paper, the author made measurements which prove that this is an excellent assumption for the 350 ms tone bursts used in this experiment [14, p.23].

Rabinowitz et al. [22] provide detailed data describing a normal hearing subject's intensity discrimination abilities at 1000 Hz as a function of overall level, furnishing the second necessary piece of information for a prediction. Figure 4-1 plots this intensity discrimination data, measured in sensitivity-per-Bel (given the symbol  $\delta'$ ), as an increasing function of level. This curve was generated by averaging data from 15 different intensity discrimination studies, and it was artificially normalized to pass through the point (40,10).

It is noted that  $\delta'$  is inversely proportional to the just-noticeable difference (JND), which is the smallest intensity difference that a subject can detect, measured in decibels. Rabinowitz et al. define



Figure 4-1: Intensity discrimination of an average normal hearing subject, measured in sensitivity-per-Bel as a function of sensation level (decibels above threshold). The stimulus is a long-duration pure tone at 1 kHz. Taken from Rabinowitz et al. (1976).



the JND to be [22]:

$$\delta'(L) = \frac{10}{\text{JND}(L)} \quad (4.1)$$

where  $\delta'$  and the JND are both functions of the overall level  $L$  of the tones.

Equation 4.1 has relevance to the expansion simulator's effects on  $\delta'$ , which can be demonstrated by examining its effects on the JND. In the recruiting region of operation, the simulator's static transfer function has a slope of  $K \neq 1$  and magnifies decibel differences at the input by a factor of  $K$  at the output. If the system's attenuating effects are ignored for the moment, then a subject with a JND of 1 decibel in the unsimulated condition will have a JND of  $\frac{1}{K}$  in the expansion-simulated condition. According to Equation 4.1, the subject's  $\delta'$  changes inversely with JND and should increase by precisely a factor of  $K$  in the expansion-simulated case. The next section will describe a prediction algorithm which takes both the attenuation and amplitude expansion properties of the simulator into account.

### Algorithm

Figure 4-2 describes an algorithm for predicting the function relating stimulus level to intensity discrimination in the expansion-simulated condition. The algorithm uses the following functions:

**sim( $L, f$ )** The expansion simulator's static input/output function of Figure 1-3. The input parameters are the level  $L$  and frequency  $f$  of a tone at the simulator's input, and the output parameter is the level at the simulator's output. The hearing loss simulated is 50 dB.

**spl2sl( $L$ )** A simple translation from sound pressure level to sensation level, using an individual subject's audiogram.

Figure 4-2: Algorithm to predict expansion-simulated intensity discrimination.

**Step 1:** choose an input intensity  $L$  to the expansion simulator.

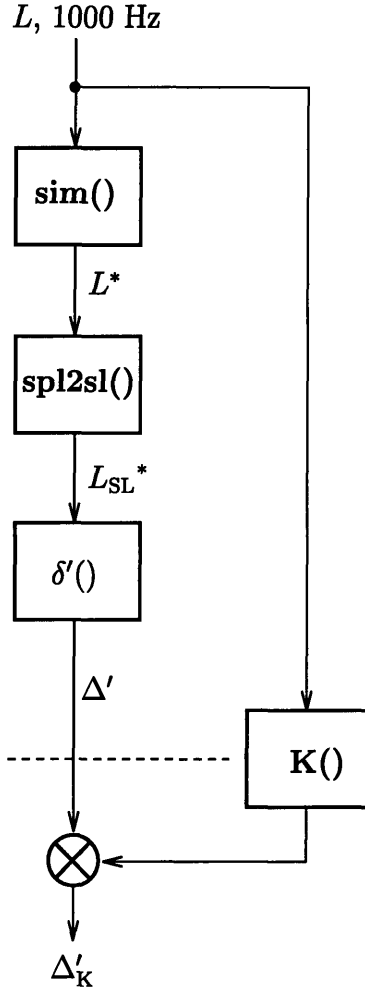
**Step 2:** find  $L^*$ , the level at the output of the simulator.

**Step 3:** find  $L_{SL}^*$ , the sensation level corresponding to  $L^*$ .

**Step 4:** Calculate the sensitivity-per-Bel at the output sensation level  $L_{SL}^*$ .

**Step 5:** Using the original input level, calculate the slope of the simulator's static transfer function.

**Step 6:** Scale up the sensitivity-per-Bel by the expansion factor of the simulator.



$\delta'(L)$  The function in Figure 4-1, which relates intensity discrimination to sensation level for a normal hearing subject (at a frequency of 1 kHz).

$K(L)$  describes the slope of the simulator's static input/output characteristic as a function of input level (at a frequency of 1 kHz).

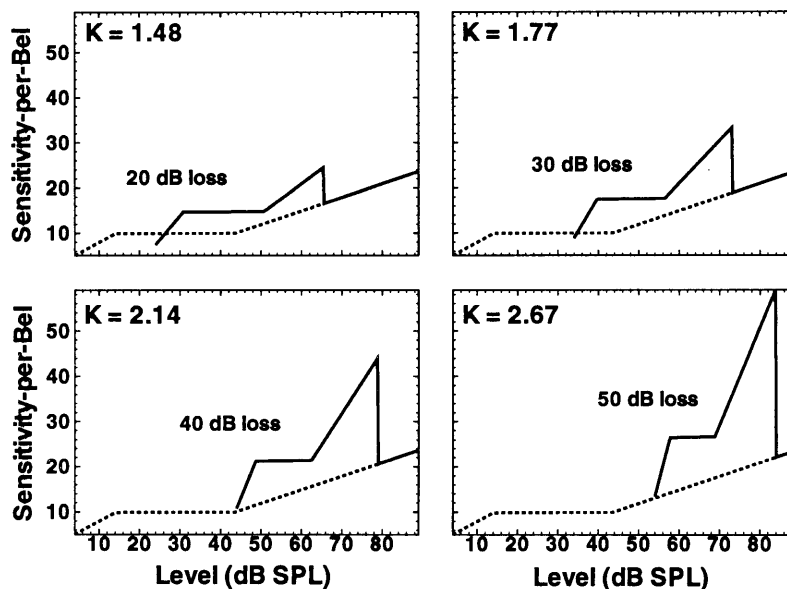
For a particular level  $L$  at the simulator's input, the level at the output is calculated to be

$$L^* = \text{sim}(L, 1000).$$

This first step accounts for the effects of the simulator's attenuation. This output level in dB SPL is then transformed into a level in dB SL to produce

$$L_{SL}^* = \text{spl2sl}(L^*).$$

Figure 4-3: Comparison of predicted intensity discrimination in the expansion simulated condition with data from normal hearing persons from Rabinowitz et al. The comparisons are made for stimuli at equal sound pressure level, with simulated losses of 20, 30, 40, and 50 dB. The dashed lines reproduce the normal data from Figure 4-1, and the solid lines are the predicted functions from the expansion simulated condition. At the top of each panel is the simulator expansion factor  $K$ .



Next the sensitivity-per-Bel at this output sensation level is determined to be

$$\Delta' = \delta'(L_{SL}^*).$$

Finally, the effects of the level-expansion must be accounted for.  $\Delta'$  must be scaled up by the slope of the simulator's transfer function at the given input level to produce the final intensity discrimination,

$$\Delta'_K = \Delta' \cdot K(L).$$

## Results

Using a hypothetical normal-hearing subject whose threshold at 1 kHz is 4 dB SPL, expansion-simulated intensity discrimination functions were predicted for flat hearing losses of 20, 30, 40, and 50 dB. Figures 4-3, 4-4, and 4-5 plot the predicted functions on the same axes as the unsimulated normal function of Rabinowitz, et al., comparing sensitivity at equal sound pressure level, sensation level, and loudness respectively.

The results predict that intensity discrimination will be *better than normal* in the expansion simulated condition when compared to that of normal hearing subjects at equal sound pressure levels, equal sensation levels, or equal loudness. The only exceptions to this rule occur in the equal

Figure 4-4: Same data as in Figure 4-3 compared at equal *sensation levels* rather than equal sound pressure levels.

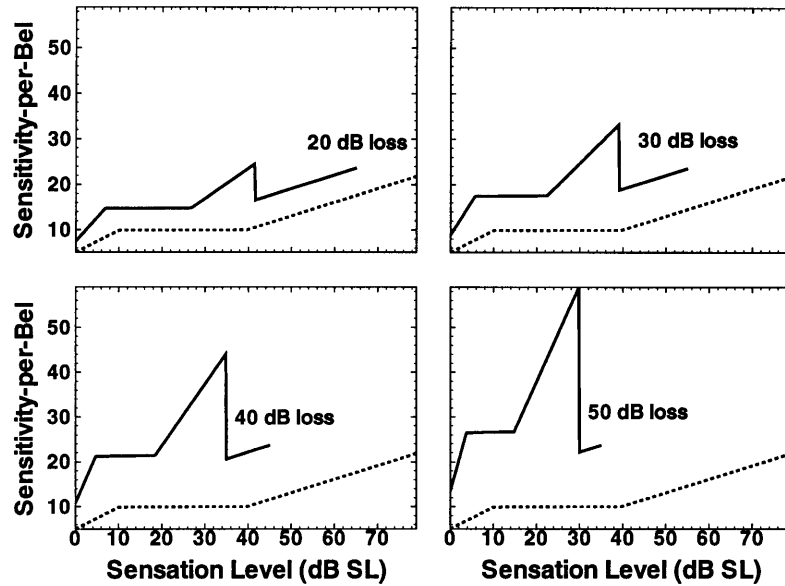


Figure 4-5: Same data as in Figure 4-3 compared at equal *loudness* rather than equal sound pressure levels. The simulator's static input/output function was used to determine points of equal loudness in the unexpanded and expansion simulated conditions.

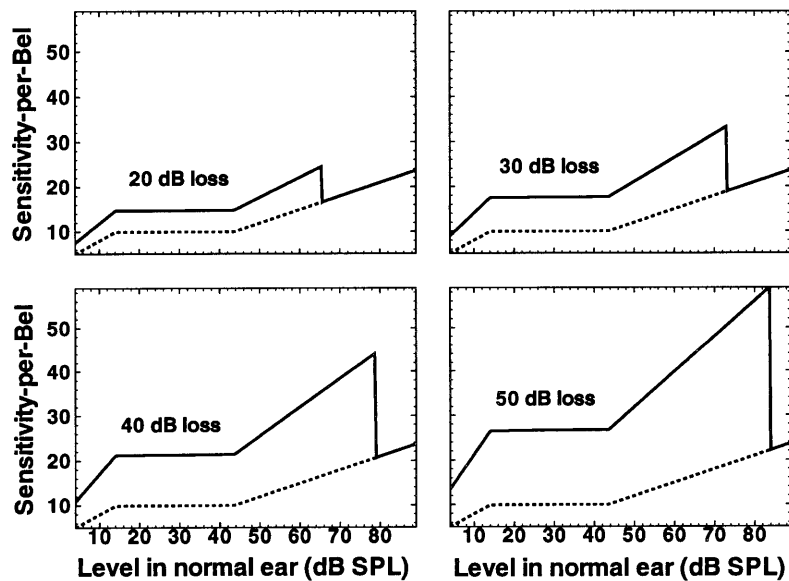
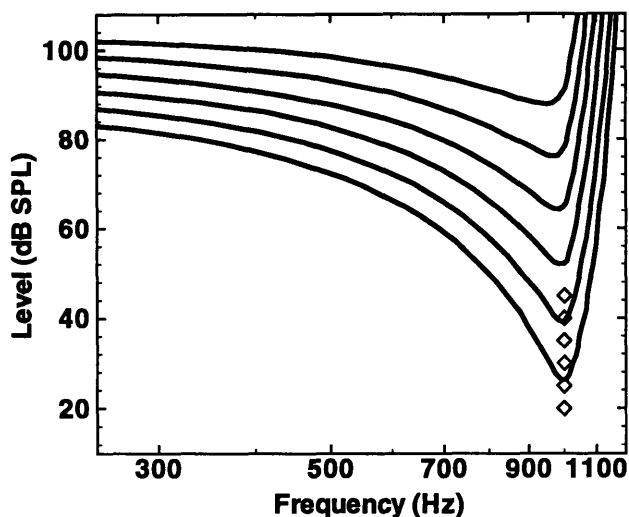


Figure 4-6: The psychophysical tuning curve, as a function of both masker frequency and probe level. Probe levels and frequency are indicated with the “◇” symbols. As the probe level increases, so does the height and broadness of the tuning curve.



SPL comparison within several decibels of impaired threshold for the simulated losses of 20 and 30 dB (top of Figure 4-3). In the equal SPL comparison, the peaks in discrimination at high levels reflect the fact that almost no attenuation is taking place there, but the expansion is having its full effect. Above the threshold of complete recruitment, the discrimination curves abruptly drop back to normal due to the restoration of unity gain in the simulator. In the equal loudness comparison, the expansion simulated predictions are everywhere a factor of  $K$  greater than the normal hearing data, where  $K$  is the expansion factor of the simulator.

## 4.2 Psychoacoustic Tuning Curves

To predict how a normal-hearing person’s PTC is affected when the expansion simulator is in place requires two things: a detailed knowledge of the function relating the shape of the PTC to probe level and masker frequency and a model of the input/output characteristic for the simulator.

Nelson et al. [17] have made measurements of PTCs at a variety of masker frequencies and probe levels while keeping the probe frequency fixed at 1 kHz. Based on their measurements and a model of auditory excitation, they have produced smooth functions relating masker level to frequency (PTCs) for a variety of probe levels. These functions are presented in Figure 4-6. As the probe level increases from 20 dB SPL to 45 dB SPL, the tuning curves elevate and broaden out. Nelson used a 4AFC procedure to determine masked thresholds for the tuning curves. Masking tones were 200 ms in duration and probe tones were 20 ms, both gated with 10 ms cosinusoidal rise and fall times. The

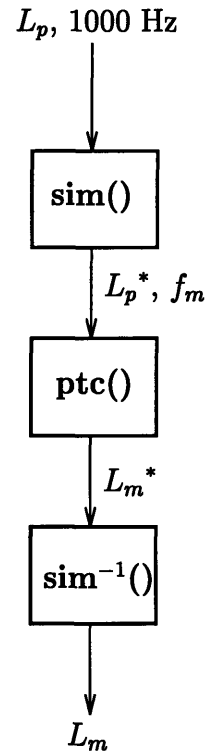
Figure 4-7: Algorithm for predicting the PTC experiment for normal-hearing subjects using the expansion hearing loss simulation.

**Step 1:** choose a 1000 Hz probe level  $L_p$  to use at the input to the expansion simulator.

**Step 2:** find  $L_p^*$ , the probe level at the output of the simulator.

**Step 3:** find  $L_m^*$ , the necessary masker level at the output of the simulator at frequency  $f_m$  to mask the probe at level  $L_p$ .

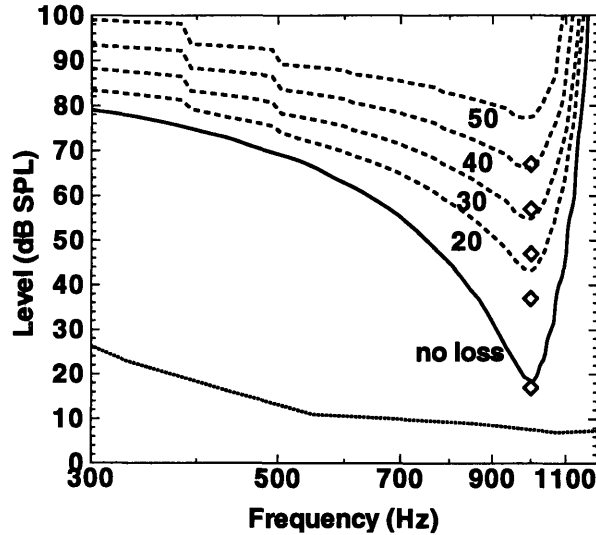
**Step 4:** using the inverse model for the simulator, find the input level  $L_m$  necessary to produce  $L_m^*$  at the output.



period between masker and probe (10% masker offset to 10% probe onset) was 2 ms.

To simplify the complex input/output characteristic of the simulator, the masker and probe tone bursts will be treated as if they were infinite in duration. The response of the simulator to infinite-duration sinusoids is easy to calculate, since all transients disappear in the steady state. It is further assumed that the consecutive masker and tone bursts have no effect on one another in terms of power estimation, i.e. that the simulator “sees” each of them individually. Of course, neither of these assumptions is strictly true: the tone bursts are far from infinite-duration, so the simulator will actually distort their shape from input to output [14, p.25]. Also, the two bursts are only separated by 2 ms of near-silence and 20 ms of rise/fall times, and since the simulator measures input power by looking at a 20 ms window of the signal, it *will* “see” them simultaneously. It is hoped that the assumptions are accurate enough to produce useful hypotheses for the outcome of the PTC experiment.

Figure 4-8: Tuning curves from a hypothetical normal-hearing subject using the expansion simulator with a variety of flat losses. The dotted line at bottom is the subject's normal threshold. The solid line is the subject's normal tuning curve, and the dashed lines represent PTCs at simulated losses of 20, 30, 40, and 50 dB. The  $\diamond$  symbols indicate the frequency and level of the probe, which is always 10 dB above the (impaired) threshold. The curves were calculated using the method of Figure 4-7.



### Algorithm

Now that the two tools are in place, the method of predicting the results of the expansion-simulated PTC experiment is straightforward. Figure 4-7 shows the steps required to predict the necessary masker level for each masker frequency and probe level. The following functions were used in the diagram:

$\text{sim}(L, f)$  The expansion simulator's static input/output function of Figure 1-3. The input parameters are the level  $L$  and frequency  $f$  of a tone at the simulator's input, and the output parameter is the level at the simulator's output. The hearing loss simulated varied from 20 to 50 dB.

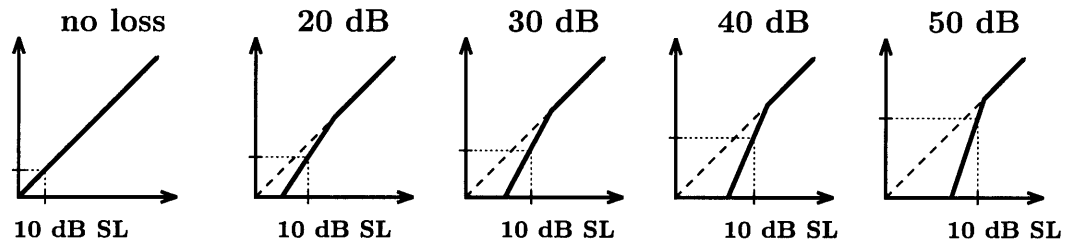
$\text{ptc}(L, f)$  The function in Figure 4-6 describing the shape of the psychophysical tuning curve as a function of probe level  $L$  and masker frequency  $f$ . Probe frequency is assumed to be 1 kHz.

$\text{sim}^{-1}(L, f)$  The inverse system of  $\text{sim}(L, f)$ . That is, it maps tone levels and frequencies at the *output* of the simulator to the tone level at the *input*.

For a given probe level  $L_p$  and masker frequency  $f_m$ , the probe level presented to the subject at the simulator output is calculated to be

$$L_p^* = \text{sim}(L_p, 1000).$$

Figure 4-9: Static input/output relations are shown for hearing losses of 0 through 50 dB. At each degree of loss, an input tone of 10 dB SL (10 dB above impaired threshold) is mapped from the input to the output, shown with dotted lines. Although the input level is maintained at 10 dB above threshold, the output level increases with the degree of hearing loss.



Using the data from Nelson, the required masker level at the simulator output is calculated to be

$$L_m^* = \text{ptc}(L_p^*, f_m).$$

Finally, the masker level at the *input* of the simulator which will produce  $L_m^*$  at the output is calculated to be

$$L_m = \text{sim}^{-1}(L_m^*, 1000)$$

and plotted in Figure 4-8.

## Results

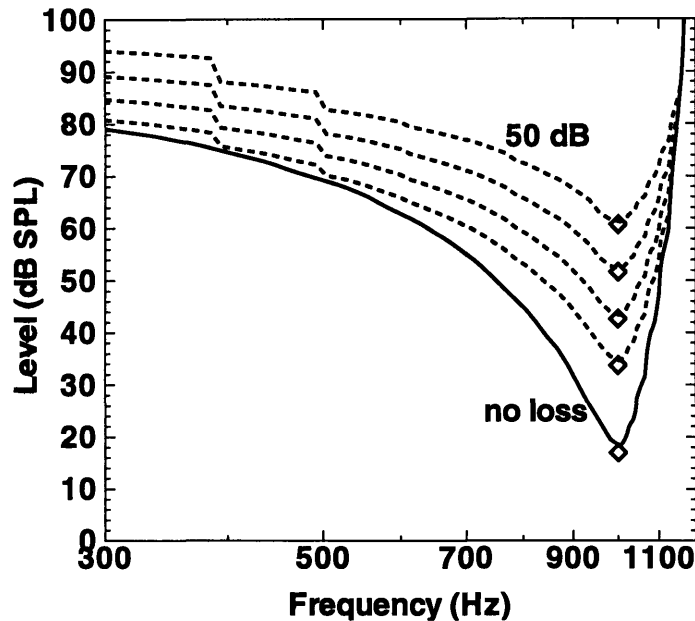
Expansion-simulated tuning curves were calculated for flat hearing losses of 20, 30, 40, and 50 dB. The hypothetical normal-hearing subject had a threshold of 7 dB SPL at 1 kHz. For all hearing losses, the probe tone was presented at 10 dB SL (10 decibels above threshold).

Figure 4-8 plots the various PTCs all on the same axis. The hypothetical normal subject's absolute threshold is plotted below the tuning curves. The level and frequency of the probe tone is indicated below each respective curve. As the amount of hearing loss increases, the PTC grows wider, and the tip becomes less sharp. These results suggest that the expansion-simulated PTCs will qualitatively resemble the neural tuning curve measured from a damaged cochlea at the top of Figure 3-2.

There are two explanations for the prediction of broader tuning curves with increasing simulated loss. One is that the probe level in the experiment is always fixed to be 10 dB above the subject's (impaired) threshold. Due to the simulator's input/output relation, an input tone which is 10 dB above the impaired threshold maps to an increasingly higher level output tone as hearing loss increases. This mapping is demonstrated schematically in Figure 4-9 for hearing losses of 0 dB (no loss), 20, 30, 40, and 50 dB. Higher probe levels at the output of the simulator *must* result in broader



Figure 4-10: Predictions of expansion simulated tuning curves using the appropriate probe tone input level in each condition to ensure that the output level remains at 17 dB SPL. The lowest (solid) PTC is predicted for no hearing loss, and the higher (dashed) ones are predicted for hearing losses of 20, 30, 40, and 50 dB.

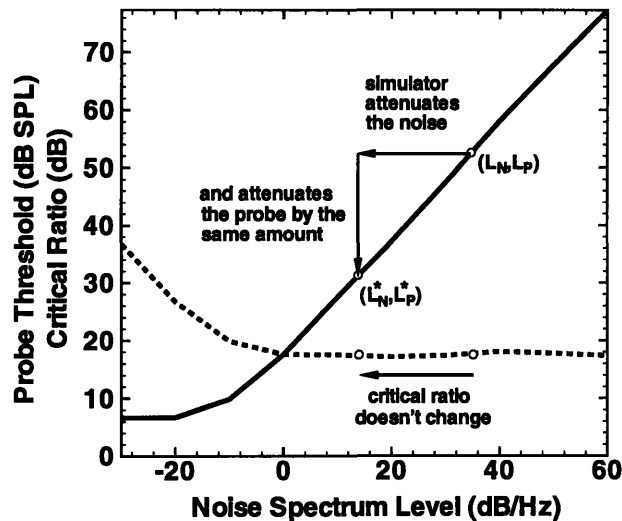


tuning curves, because the data of Nelson in Figure 4-6 shows that the higher the probe level, the broader the tuning curve.

The other explanation for the broadened tuning curves is also due to the simulator's expansive input/output relation, but it has nothing to do with increased probe levels. Suppose that in the unsimulated condition a masker must be 30 dB higher than the probe in order to mask it. In the expansion simulated condition with an expansion factor of 2, a difference of only 15 dB at the input will result in the required 30 dB difference at the output. The tuning curve's *depth* is reduced by a factor of 2, broadening it out. This explanation suffices for cases in which the probe and masker are in separate analysis bands of the system. When masker and probe share the *same* analysis band, the situation changes. The presence of the masker signal in the probe's band increases the overall power in the band, thereby reducing the amount of applied attenuation. Less attenuation means that the output probe level is higher; as explained in the previous paragraph, a higher probe level naturally results in broader tuning curves.

It is possible to study the second explanation in isolation from the first one by taking care to ensure that the output (headphone) level of the probe remains the same in both the unsimulated and expansion simulated conditions. Rather than presenting the probe at 10 dB SL for all conditions, it is presented at whatever level is required to produce a signal at the headphones which is 10 dB

Figure 4-11: Probe threshold and critical ratio at 1000 Hz as a function of noise spectrum level. The solid line is the probe threshold as a function of noise level, and the dashed line is the critical ratio, defined as the difference between the masked threshold and the noise spectrum level at that threshold. The masked threshold function is asymptotic to the probe's threshold in quiet (7 dB SPL) as the noise level decreases to inaudibility. The effects of the expansion simulator are shown on the right: with noise and probe input levels ( $L_N, L_P$ ), the output levels ( $L_N^*, L_P^*$ ) will still be on the masked threshold function, so the critical ratio will not change.



above the *unsimulated* threshold. Using this approach, Figure 4-10 displays predicted tuning curves for hearing losses of 0, 20, 30, 40, and 50 dB. The probe level is always chosen to produce a simulator output probe level of 17 dB SPL (the input levels used in the expansion simulated conditions were 33.7, 42.7, 51.1, and 60.7 dB SPL). The predicted PTCs *still* broaden out as hearing loss increases, proving that the broadening Figure 4-3 was not entirely due to increased probe levels.

### 4.3 Simultaneous Masking

To predict the effects of the expansion simulator on broad band noise masked thresholds requires data to describe a normal hearing person's masked thresholds as a function of noise level. Hawkins and Stevens provide this data, describing masked threshold as a function of both probe tone frequency and noise spectrum level for normal hearing persons [12]. Figure 4-11 plots this data for a probe at 1 kHz as a function of noise spectrum level alone. In addition, the critical ratio is computed from the masked threshold and presented as a dashed line. The relationship between probe level  $L_P$  and noise spectrum level  $L_N$  is linear with a slope of unity over almost the entire function, whose domain ranges from inaudible noise (< -10 dB/Hz) to uncomfortably loud noise (60 dB/Hz). Only

Figure 4-12: Iterative algorithm to predict the result of the critical ratio experiment. Tone frequency is set at 1 kHz.

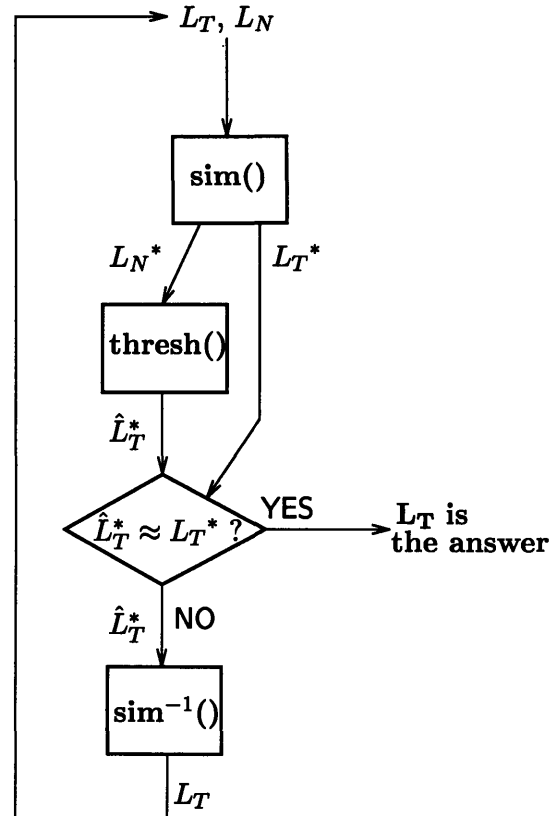
**Step 1:** choose a noise level  $L_N$  and guess an initial probe level  $L_T$  to use as inputs to the expansion simulator.

**Step 2:** find  $L_T^*$  and  $L_N^*$ , the probe and noise levels at the output of the simulator.

**Step 3:** find  $\hat{L}_T^*$ , the tone threshold at the *output* of the simulator, given the output noise level.

**Step 4:** Compare the tone level  $L_T^*$  with the true threshold  $\hat{L}_T^*$  for approximate equality.

**Step 5:** if not equal, calculate the simulator input level  $L_T$  which would result in the desired output level  $\hat{L}_T^*$ , and use it in the next iteration.



at nearly-inaudible noise levels does the function become nonlinear and asymptotic to the subject's tone threshold in quiet (7 dB SPL in Figure 4-11).

Due to the relationship between  $L_P$  and  $L_N$ , the critical ratio is nearly a constant over most of the range of noise audibility (-10 dB/Hz to 60 dB/Hz). This suggests that the effects of the expansion simulator on the critical ratio will probably be minimal. Whatever attenuation the simulator applies to the signal will be applied equally to the probe tone and the noise: input levels  $L_P$  and  $L_N$  will be reduced by the same amount, producing output levels  $L_P^*$  and  $L_N^*$  for which the critical ratios  $(L_P - L_N)$  and  $(L_P^* - L_N^*)$  are nearly identical. Figure 4-11 shows this effect graphically (see caption for details).

### Algorithm

Experimental masked thresholds for the expansion simulated condition were predicted using a hypothetical subject whose unsimulated masked threshold in noise is defined by Figure 4-11. Flat

hearing losses at 1000 Hz of 20, 30, 40, and 50 dB were simulated, and the results of the critical ratio experiment were predicted by means of the algorithm in Figure 4-12. In this algorithm, a new function is defined:

**thresh( $L_N$ )** Returns the masked threshold of a 1 kHz tone in wide band noise with a spectrum level of  $L_N$  dB/Hz. This is the function plotted in Figure 4-11.

The first step of the algorithm is to choose a noise level  $L_N$  at which to work and *guess* an initial masked threshold for the probe  $L_T$  to use at the input to the expansion simulator. A good guess is probably the  $L_T$  predicted by Hawkins and Stevens for the chosen  $L_N$ , but this will not be exactly the correct level due to the effects of the simulator. The algorithm in Figure 4-12 begins with a guess and iterates to the solution.

After choosing  $L_T$ , the next step is to calculate  $L_T^*$  and  $L_N^*$ , the probe and noise levels at the simulator output. The probe and noise are assumed to be uncorrelated, so that the tone power and the noise power contained in the same simulator band add to produce a joint level  $L_J$ , resulting in a tone output level

$$L_T^* = \text{sim}(L_J, 1000).$$

The noise in the same band as the tone is attenuated by the same amount that the tone was, so that

$$L_N^* = L_N - (L_T - L_T^*).$$

Now that the noise level at the simulator output has been determined, it may be used in conjunction with the data in Figure 4-11 to determine what the level of the probe tone *should* be in order to be at threshold. This “proper” probe level  $\hat{L}_T^*$  is computed to be

$$\hat{L}_T^* = \text{thresh}(L_N^*).$$

The *actual* probe level that resulted from the guess in step 1 is then compared to the “proper” masked threshold. If the two are approximately equal, then the algorithm has converged to the solution. If not, then the next step is to repeat step 1 with a new guess for  $L_T$ .

The algorithm closes in on the correct  $L_T$  by using the inverse simulator function,  $\text{sim}^{-1}()$  to provide the next guess. Based on what the probe’s masked threshold *should* have been ( $\hat{L}_T^*$ ), the next guess is calculated to be

$$L_T = \text{sim}^{-1}(\hat{L}_T^*, L_J^*),$$

where  $L_J^*$  is the total power contained at the *output* of the simulator in the band containing a tone at  $\hat{L}_T^*$  and noise at  $L_N^*$ . The algorithm proceeds until convergence, which typically happens after 2 iterations.

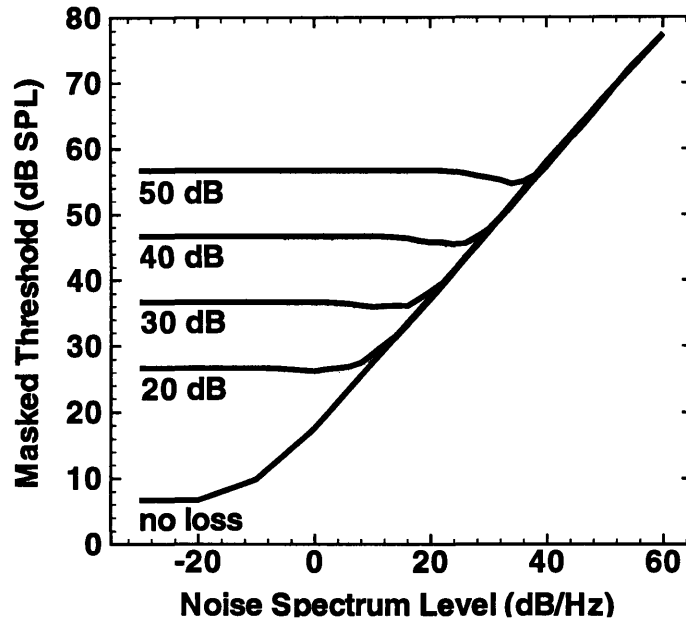


Figure 4-13: Predicted masked thresholds in wide band noise as a function of noise level for a variety of simulated losses.

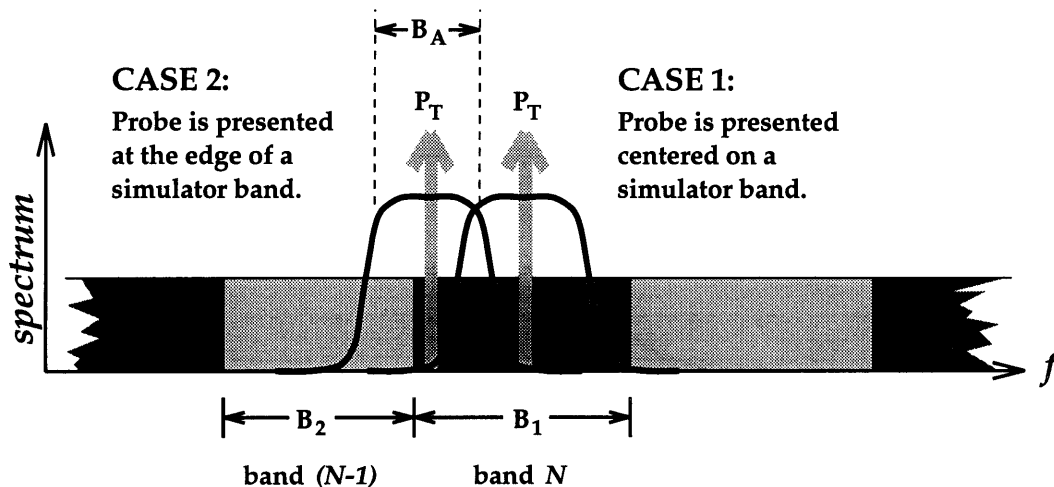
## Results

Plots of masked threshold versus noise level generated with the above algorithm are shown in Figure 4-13. As expected, the noise masked thresholds do not change noticeably in the simulated conditions, except when the probe's masked threshold drops beneath the simulated impaired threshold. Interestingly, the function relating noise power to masked threshold has acquired an inflection point; it is no longer monotonic. For an explanation, consider the top curve in Figure 4-13 pertaining to a simulated 50 dB loss. The hypothetical subject's absolute threshold in this condition is 57 dB SPL, but for a range of masking noise levels ( $28 \text{ dB/Hz} \leq P_N \leq 40 \text{ dB/Hz}$ ) the predicted masked threshold drops *below* absolute threshold. Apparently the additional power supplied by the masking noise decreases the attenuation in the probe's simulator band enough to raise a normally inaudible tone into the audible region.

## Filterbank Effects

As discussed in Section 1.1.3, the expansion simulator processes the input signal in many independent frequency bands. The prediction in the previous section made the implicit assumption that the probe and noise portions of the signal were attenuated by the same amount during simulation, but this is only true if the probe and the band of noise responsible for masking it fall into the same frequency band. This assumption may break down if the probe tone is positioned close to the edge of a

Figure 4-14: Effects of the bandpass nature of the expansion simulator in the simultaneous masking experiment. In Case 1, the probe tone (and auditory filter) is *centered* on one of the simulator's bandpass filters, which are depicted by alternating light and dark rectangles. In Case 2, the tone is placed at the very edge of one of the filters. As a result of the placement of the tone, different critical ratios may be measured.



frequency band.

Figure 4-14 illustrates how the assumption of identical probe and noise processing in the masked threshold experiment can break down (see caption for explanation). In Case 1, the probe is centered on the simulator band, and in Case 2 it is positioned at the very edge of a band.

To determine a quantitative difference in the masked thresholds of Cases 1 and 2, the SNR at the “output” of the auditory filter will be calculated for each case and compared. Let simulator bandpass filter  $N$  (from Figure 4-14) have bandwidth  $B_1$ , filter  $(N - 1)$  have bandwidth  $B_2$ , and the approximately-rectangular auditory filter have bandwidth  $B_A$ . Let the power per Hertz of the input noise be  $P_N$  and the power of the input probe tone be  $P_T$ . Finally, let the function  $\mathcal{A}_1(\cdot)$  relate power in simulator band  $N$  to the attenuation applied to that band, and let  $\mathcal{A}_2(\cdot)$  describe the same relation for band  $(N - 1)$ . It is emphasized that all of the powers, bandwidths, attenuations, and SNRs dealt with in this section are absolute numbers, not decibel values.

First consider Case 1. The ear's auditory filter is completely contained within band  $N$  of the simulator as shown in Figure 4-14, so only signals and noise contained in this band need be considered. Entering band  $N$  of the simulator are both a signal component (the probe) and a noise component (the masking noise contained within the band). The amounts of power contained in these signal and noise components are

$$P_T \quad \text{and} \quad B_1 P_N.$$

Assuming that these signal and noise components are uncorrelated, their powers add, and the total power entering simulator filter  $N$  is

$$P_1 = P_T + B_1 P_N.$$

Due to the simulator's attenuative effects on an input with power  $P_1$ , the signal and noise components at the *output* of the system have respective powers

$$\mathcal{A}_1(P_1) \cdot P_T \quad \text{and} \quad \mathcal{A}_1(P_1) \cdot B_1 P_N.$$

The masker and probe then pass through the auditory filter, which passes the tone completely but selects only a fraction of the noise. The signal and noise components at the output of the auditory filter become

$$\mathcal{A}_1(P_1) \cdot P_T \quad \text{and} \quad \mathcal{A}_1(P_1) \cdot B_1 P_N \frac{B_A}{B_1},$$

resulting in an SNR of

$$\text{SNR}_1 = \frac{\mathcal{A}_1(P_1) \cdot P_T}{\mathcal{A}_1(P_1) \cdot B_1 P_N \frac{B_A}{B_1}} = \frac{P_T}{P_N B_A}. \quad (4.2)$$

Next, consider Case 2. In this case it is no longer true that the auditory filter is entirely contained within band  $N$ : half of it is in band  $N$  and half of it is in band  $(N - 1)$ . Therefore, the signal and noise components in *both* of these bands need to be considered.

The signal and noise power entering band  $N$  are the same as in Case 1, so an equal attenuation will be applied to that band. However, because only half of the auditory filter is now in band  $N$ , only half as much noise passes through it as compared with Case 1. The powers of the signal and noise components at the output of the auditory filter from simulator band  $N$  are now

$$\mathcal{A}_1(P_1) \cdot P_T \quad \text{and} \quad \mathcal{A}_1(P_1) \cdot B_1 P_N \frac{B_A}{2B_1}. \quad (4.3)$$

Now consider band  $(N - 1)$  in Case 2. There is no probe signal entering this band, but the amount of noise power entering it is

$$P_2 = B_2 P_N.$$

Simulator attenuation produces an output noise power of

$$\mathcal{A}_2(P_2) \cdot B_2 P_N,$$

which is further filtered by the auditory filter to produce a final noise component due to band  $(N - 1)$  with power equal to

$$\mathcal{A}_2(P_2) \cdot B_2 P_N \frac{B_A}{2B_2}. \quad (4.4)$$

For Case 2 the signal component from Equation 4.3 and the noise components from Equations 4.3 and 4.4 result in an overall SNR at the output of the auditory filter of

$$\text{SNR}_2 = \frac{\mathcal{A}_1(P_1) \cdot P_T}{\frac{1}{2} [\mathcal{A}_1(P_1) \cdot B_A P_N + \mathcal{A}_2(P_2) \cdot B_A P_N]} = \frac{2\mathcal{A}_1(P_1) \cdot P_T}{B_A P_N [\mathcal{A}_1(P_1) + \mathcal{A}_2(P_2)]}. \quad (4.5)$$

Degree of Hearing Loss dB	Noise Spectrum Level (dB/Hz)			
	20	30	40	50
20	0.6	0.6	0.6	0
30	1.0	1.0	1.0	1.0
40	0	1.3	1.3	1.3
50	0	0	1.8	1.8

Table 4.1: Size of the filterbank effect, in decibels, for simulated hearing losses between 20 and 50 dB and four noise levels.

Comparing Equations 4.2 and 4.5, it is clear that the SNR in case 2 may easily be expressed in terms of the SNR in case 1:

$$\text{SNR}_2 = \left( \frac{2\mathcal{A}_1(P_1)}{\mathcal{A}_1(P_1) + \mathcal{A}_2(P_2)} \right) \text{SNR}_1. \quad (4.6)$$

### Relevance of Filterbank Effects

Equation 4.6 predicts that different SNRs will exist at the output of the ear's auditory filter in Cases 1 and 2. Therefore, the filterbank nature of the simulator may show up as an artifact in the masked threshold experiment. However, it is also possible that the filterbank effect is so small that it will not be noticed. This section estimates the size of the effect.

Equation 4.6 has shown that the signal-to-noise ratios in Cases 1 and 2 differ by a factor  $F$ , where

$$F = \frac{2\mathcal{A}_1(P_1)}{\mathcal{A}_1(P_1) + \mathcal{A}_2(P_2)}.$$

The functions  $\mathcal{A}_1(\cdot)$  and  $\mathcal{A}_2(\cdot)$  are attenuations applied by the simulator; as such, their ranges must be contained in the interval  $[0, 1]$ . Inspection shows that the only possible values for the factor  $F$  are on the interval  $[0, 2]$ . Knowledge of the relative sizes of  $\mathcal{A}_1(P_1)$  and  $\mathcal{A}_2(P_2)$  puts further constraints on the value of  $F$ :

$$\mathcal{A}_1(P_1) > \mathcal{A}_2(P_2) \implies 1 \leq F \leq 2 \quad (4.7)$$

$$\mathcal{A}_1(P_1) < \mathcal{A}_2(P_2) \implies 0 \leq F \leq 1 \quad (4.8)$$

As long as the bandwidth of simulator band  $N$  is approximately equal to the bandwidth of simulator band  $(N - 1)$  then band  $N$  must contain more power than band  $(N - 1)$  because it contains the probe tone as well as the same noise power. Assuming that the input/output functions in bands  $N$  and  $(N - 1)$  are nearly identical, then the more powerful band  $N$  will receive *less* attenuation, so that

$$\mathcal{A}_1(P_1) > \mathcal{A}_2(P_2). \quad (4.9)$$

Together, Equations 4.7 and 4.9 dictate that  $F$  fall into the range  $[1, 2]$ . The signal-to-noise ratio



in Case 2 is between 1 and 2 times better than that of Case 1. Therefore, in Case 2 an experimenter can expect to see a decrease in masked threshold of up to 3 dB with respect to Case 1.

Table 4.1 presents the results of calculations to determine the exact size of the filterbank effect for various noise levels and various degrees of loss. In the calculations, band  $N$  of the simulator was the 265-Hz wide filter band centered on 1074 Hz (containing the 1000 Hz probe) and band  $(N - 1)$  was the 155-Hz wide filter band centered on 854 Hz<sup>1</sup>. Probe tones were assumed to be at 1000 Hz for Case 1 and 945 Hz for Case 2. The figures in Table 4.1 refer to the decibel difference between SNR2 and SNR1.

The filterbank effect is expected to increase with the degree of simulated loss, but it should never exceed 2 dB. The numbers in Table 4.1 are even slightly exaggerated due to the assumption that the auditory filter in Case 1 is entirely included in band  $N$  of the simulator. In the prediction, with a probe tone at 1000 Hz, the auditory filter centered at 1000 Hz is only 60 Hz away from the edge of band  $N$  (the 941–1206 Hz band). A normal hearing subject's auditory filter may be wider than 120 Hz at 1000 Hz [10], in which case the assumption will break down and reduce the size of the effect.

### 4.3.1 Two Tone Suppression

Experiments with simulated hearing loss were *not* performed, as further explained in Section 5.4. Based on the results of preliminary unsimulated experiments, it was decided that nothing would be gained by measuring suppression with simulated hearing loss. As a consequence, predictions of the expansion simulated condition were not made.

---

<sup>1</sup>For more detailed information on the simulator's filterbank, see Lum [14, p.15].

## Chapter 5

# Experimental Results

Each section of this chapter will present the data from an expansion-simulated experiment alongside its predicted outcome from Chapter 4. The noise simulated results will also be shown for purposes of comparison. In all figures, theoretical predictions and normal hearing data from the literature appear as smooth lines. Data from the three experimental conditions is plotted with symbols: “ $\diamond$ ” for the unsimulated condition, “ $\circ$ ” for the expansion simulated condition, and “ $\triangle$ ” for the noise simulated condition.

### 5.1 Intensity Discrimination

According to Rabinowitz et al., different experimental paradigms and parameter values can lead to substantially different absolute values of  $\delta'$ . However, they assume that the *shape* is always the same, so that a multiplicative constant may be used as a fitting parameter. Accordingly, the experimental data from the unsimulated condition was fit to the normal hearing data from Rabinowitz et al. by means of a scale factor. The scale factor was chosen so as to best fit the experimental data to Rabinowitz et al. using the total summed magnitude of error as a fitting criterion. The same scale factor was then applied to both the expansion simulated data and the noise simulated data.

For each subject two figures are presented: the first shows the experimental results from all three conditions, compared at equal sound pressure levels. In this figure, the normal hearing data from Rabinowitz et al. and the expansion simulated predictions from Chapter 4 are also shown on the same set of axes. The second figure compares the results of the three conditions at both equal sensation levels and equal loudness levels. Points of equal loudness for the expansion simulated case and unsimulated case were assumed to lie on the static input/output characteristic of the simulator. The same assumption was made for loudness in the noise simulation. The simulated hearing loss in the experiments was 50 dB.

Appendix A discusses how the data was transformed from percent correct measurements into

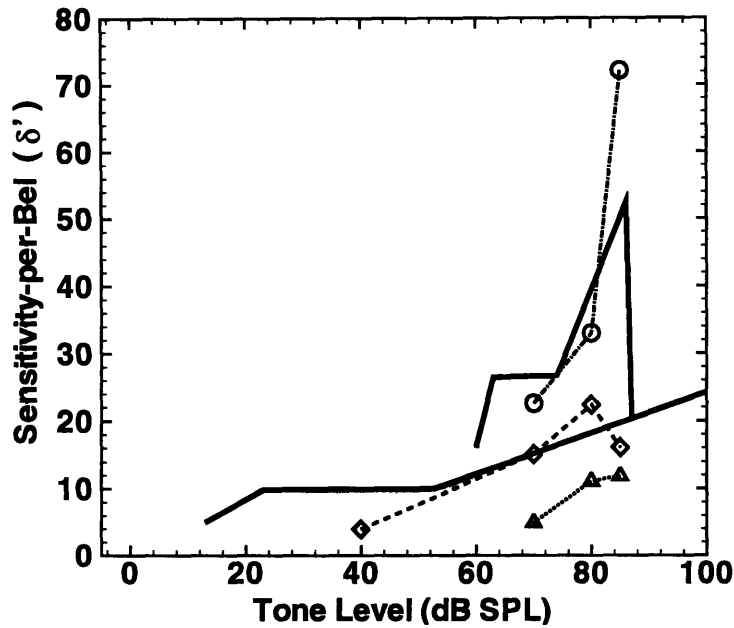


Figure 5-1: Predictions and experimental data from the intensity discrimination experiment for subject JW; the three conditions are compared at equal sound pressure levels. Solid lines are the data from Rabinowitz et al. (bottom) and the expansion simulated prediction with a simulated flat 50 dB loss (top). Symbols are the data from the unsimulated case ( $\diamond$ ), expansion simulated case ( $\circ$ ), and noise simulated case ( $\triangle$ ).

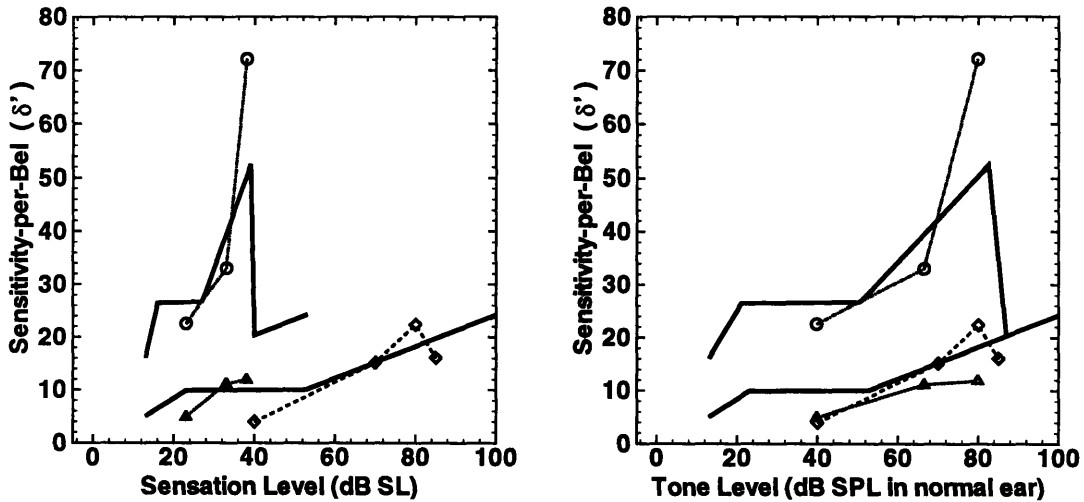


Figure 5-2: These two panels contain the same data for JW as in Figure 5-1, but instead of comparing the three conditions at equal sound pressure levels, they are compared at equal *sensation levels* (left) and *equal loudness* (right). The legend is the same as in the previous figure.

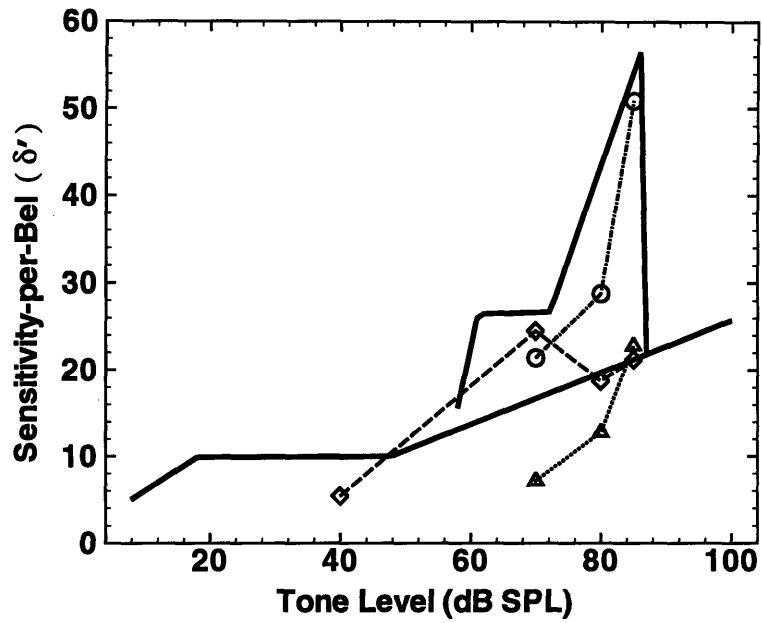


Figure 5-3: Predictions and experimental data from the intensity discrimination experiment for subject KL. Legend is the same as in Figure 5-1.

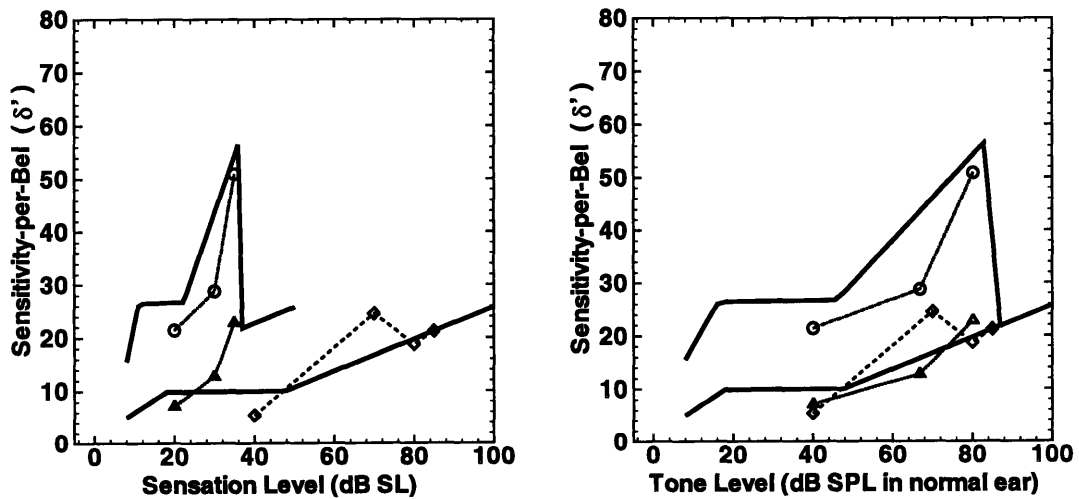


Figure 5-4: These two panels contain the same data for KL as in Figure 5-3, but instead of comparing the three conditions at equal sound pressure levels, they are compared at equal *sensation levels* (left) and *equal loudness* (right). The legend is the same as in the previous figure.

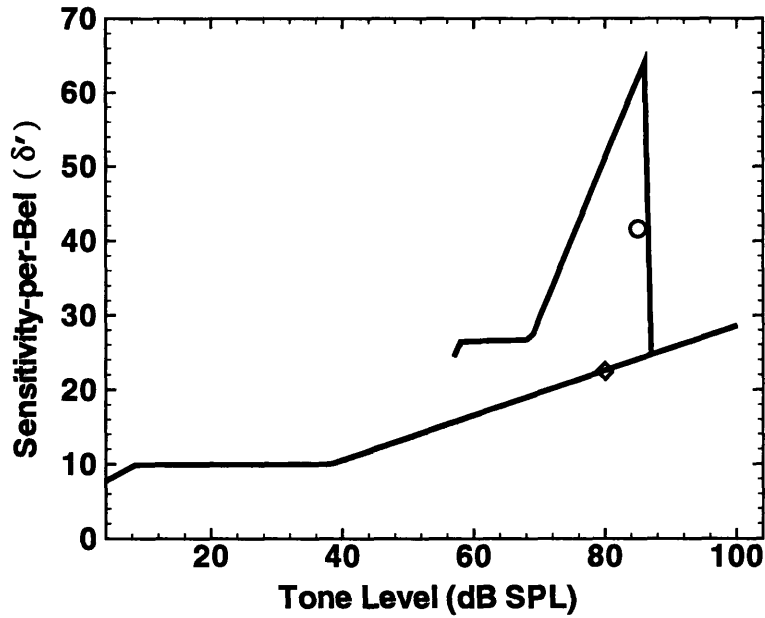


Figure 5-5: Predictions and experimental data from the intensity discrimination experiment for subject JL. Legend is the same as in Figure 5-1.

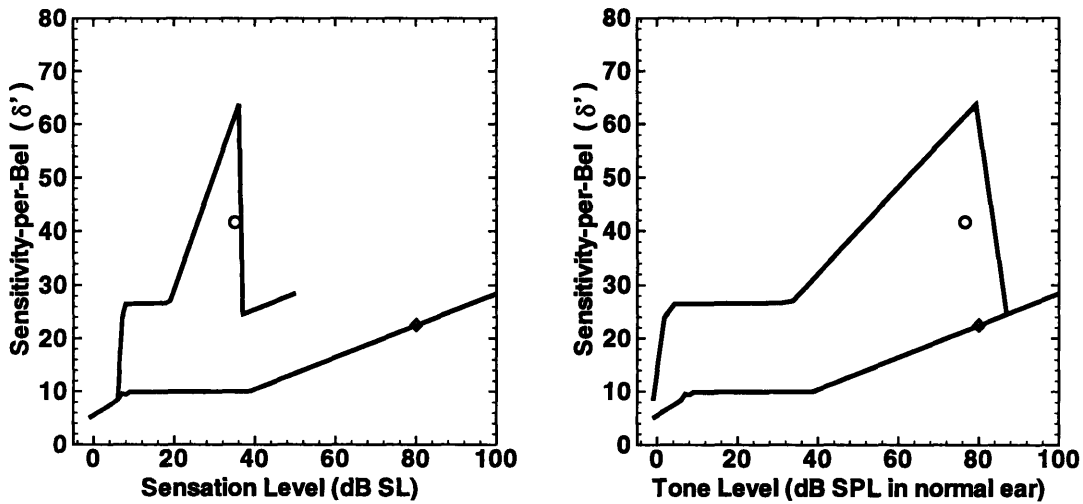


Figure 5-6: These two panels contain the same data for JW as in Figure 5-3, but instead of comparing the three conditions at equal sound pressure levels, they are compared at equal *sensation levels* (left) and *equal loudness* (right). The legend is the same as in the previous figure.

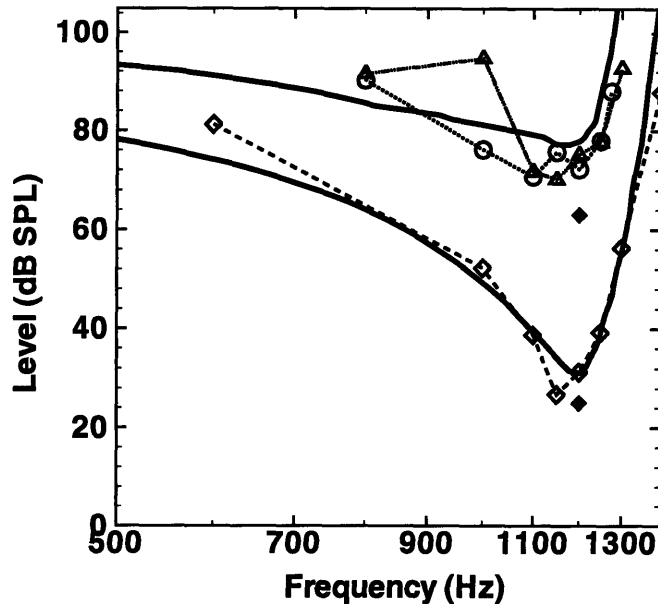


Figure 5-7: Predictions and experimental data from the PTC experiment with subject DL. The solid lines are the *predicted* PTCs in the unsimulated condition (bottom) and with an expansion simulated flat loss of 40 dB (top). Symbols show the data from the unsimulated case (◇), expansion simulated case (○), and noise simulated case (△). The level and frequency of the probe in the unsimulated and simulated cases is given by the filled ◆ symbols.

sensitivity-per-Bel.

## 5.2 Psychophysical Tuning Curves

Comparing the psychophysical tuning curve predictions of Chapter 4 with the experimental PTC data required two kinds of fitting. First, an adjustment had to be made to account for the different probe frequencies: the data from Nelson which was used to make the predictions was generated using probe tones at 1000 Hz, but the experimental data was generated using probe tones at 1200 Hz. To compensate for this mismatch, the frequency axis of the predicted curves was scaled up by a factor of  $\frac{1200}{1000}$  before any comparisons were made.

The second kind of fitting was done to account for intersubject variability. Unsimulated PTCs from DL and AM were not a good match to the normal tuning curves predicted by Nelson et al. at equal probe levels. To ensure that at least the *unsimulated* data matched its model as closely as possible, the set of tuning curves in Figure 4-6 was linearly shifted up or down so as to best fit each subject's data at the experimental probe level. The fitting criterion used was the total summed magnitude of error. When specific predictions were made for AM and DL in the expansion simulated case, the *shifted* tuning curve models were used for prediction rather than the original data.

Figures 5-7 and 5-8 plot experimental psychophysical tuning curves for DL and AM with symbols

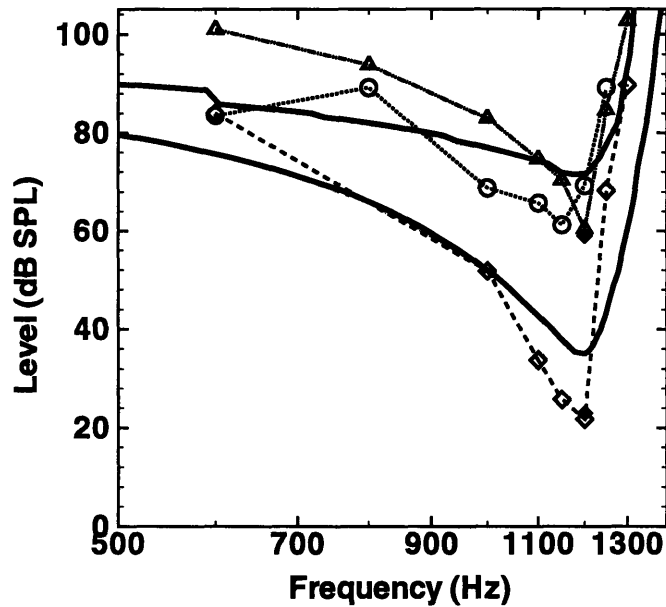


Figure 5-8: Predictions and experimental data from the PTC experiment with subject AM. The legend is the same as in Figure 5-7.

and the predictions of the expansion simulated PTCs with solid lines. Broken lines were used to connect the experimental data points together.

### 5.3 Simultaneous Masking

For the simultaneous masking experiment, comparing the experimental masked thresholds with the predicted values required only one kind of fitting. The masked threshold data from Hawkins and Stevens in Figure 4-11 was used to make predictions, but the *absolute* threshold in that data was at 7 dB SPL. Absolute thresholds for JL, KL, and JW were -1, 8, and 13 dB SPL respectively. In order to achieve accurate predictions of masked threshold near the absolute threshold, the data from Hawkins and Stevens was modified to fit the absolute threshold of each subject before the predictions were made. The modification involved lengthening or shortening the linear part of the function to achieve a new absolute threshold, but leaving the nonlinear asymptotic section unaltered.

Figures 5-9, 5-10, and 5-11 show the results of the critical ratio experiments for the JW, KL, and JL, plotted on the same axes as the predictions from Chapter 4. Threshold-fitted data from Hawkins and Stevens is shown as a solid line, and the prediction for the expansion simulated case is shown as a dashed line. Experimental data is represented by symbols. The simulated hearing loss was 40 dB.

Figures 5-12 and 5-13 from JW and KL show the effect of changing the frequency of the probe tone so as to move it from near the edge of the simulator's bandpass filter (small symbols) to near

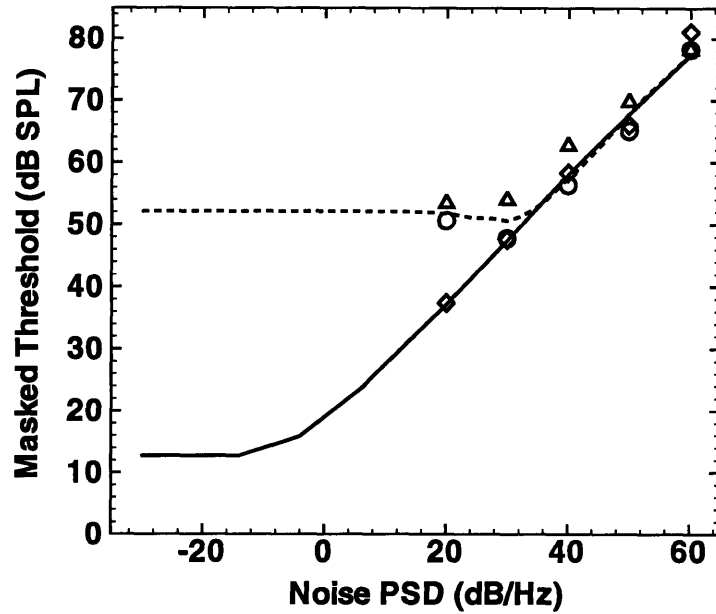


Figure 5-9: Predictions and experimental data from the simultaneous masking experiment for subject JW. Lines are the threshold-fitted Hawkins and Stevens data (solid) and the prediction of the results of an expansion-simulated 40 dB loss (dashed). Symbols show data from the un-simulated condition (◇), expansion simulated condition (○), and noise simulated condition (△).

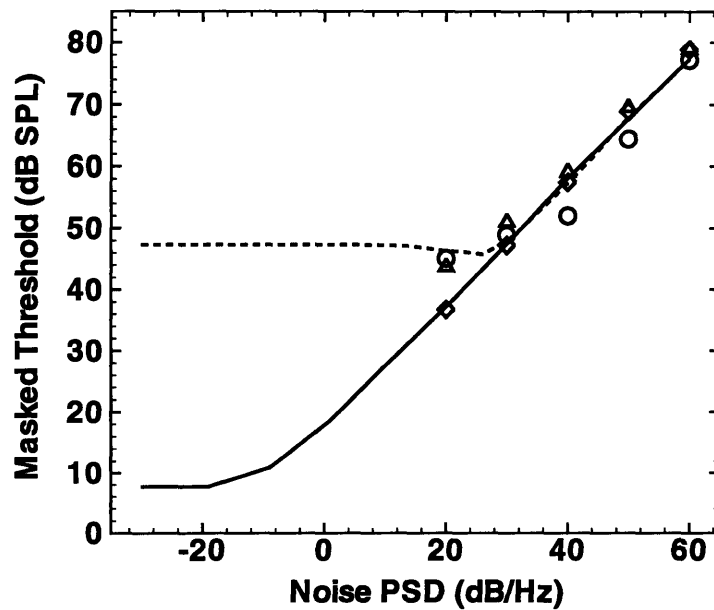


Figure 5-10: Predictions and experimental data from the critical ratio experiments for subject KL. Legend is the same as for Figure 5-9.



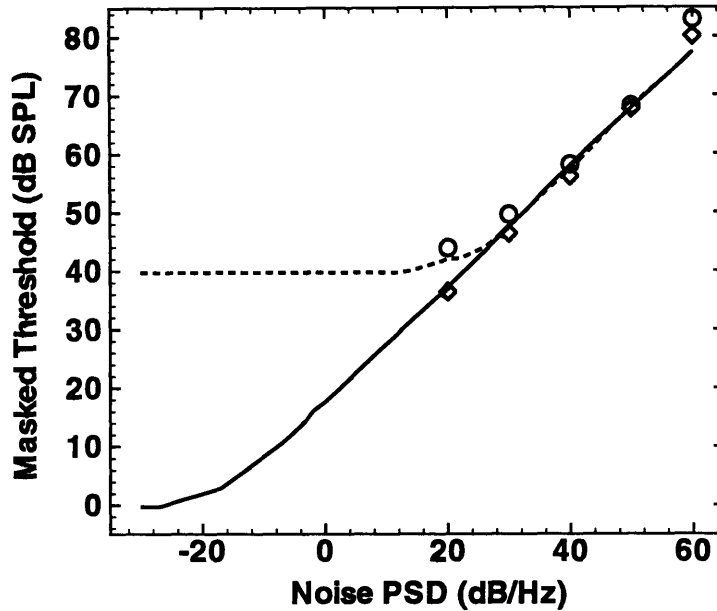


Figure 5-11: Predictions and experimental data from the critical ratio experiments for subject JL. Legend is the same as for Figure 5-9.

the center (large symbols). If the filterbank effect predicted in Section 4.3 is relevant, then it should be visible in these figures. Because the bandpass filters in the simulator are not ideal, there is some rolloff at the edges. The masked threshold data in the figures has been altered to correct for this rolloff, e.g. at 945 Hz the 941–1206 Hz filter is applying 2.4 dB of attenuation, so all of the data points at that frequency have been lowered by 2.4 dB.

## 5.4 Two Tone Suppression

The results of the suppression experiment were not what had been expected. The assumption had been that the normal hearing subjects would display a substantial amount of suppression in the unsimulated condition, verifying the results of Shannon [23] and Wightman et al. [7, p.296]). The normal suppression was to be compared against unknown expansion simulated results.

However, the results of the unsimulated experiments did *not* show a large amount of suppression in any of seven subjects tested. Figures 5-14 and 5-15 show the suppression data averaged over all subjects, using probe tones of 1 kHz and 2 kHz, respectively. Plotted on the same axes are results reported by Shannon, which show nearly 10 dB of suppression. In both figures, amount of masking is plotted as a function of suppressor frequency; negative values indicate suppression.

As Figures 5-14 and 5-15 show, the average amount of suppression demonstrated by the subjects in this thesis never exceeded 3 dB. It was decided that the effects of the hearing loss simulations on such a small amount of suppression was likely to be inconclusive, so the expansion and noise

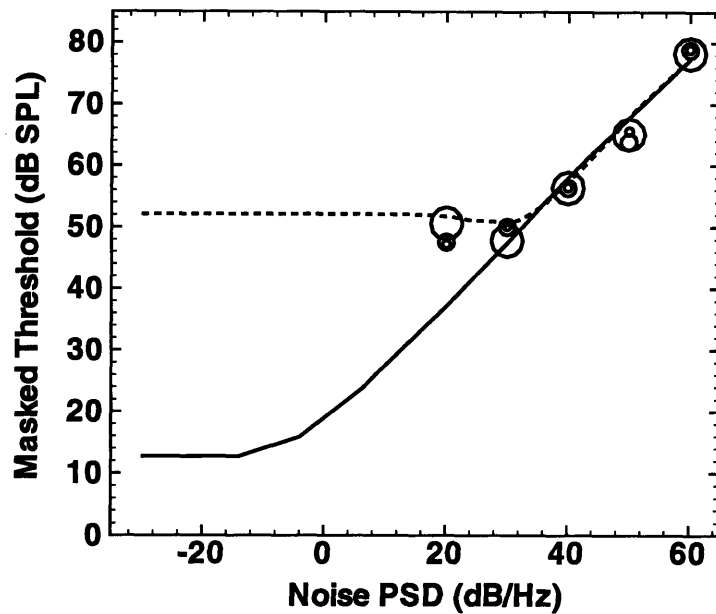


Figure 5-12: Filterbank effects of changing the probe frequency in the expansion simulated condition for subject JW. Symbol size increases as the frequency increases from the extreme edge of the band (945 Hz) to nearer the center (955 Hz and 1000 Hz).

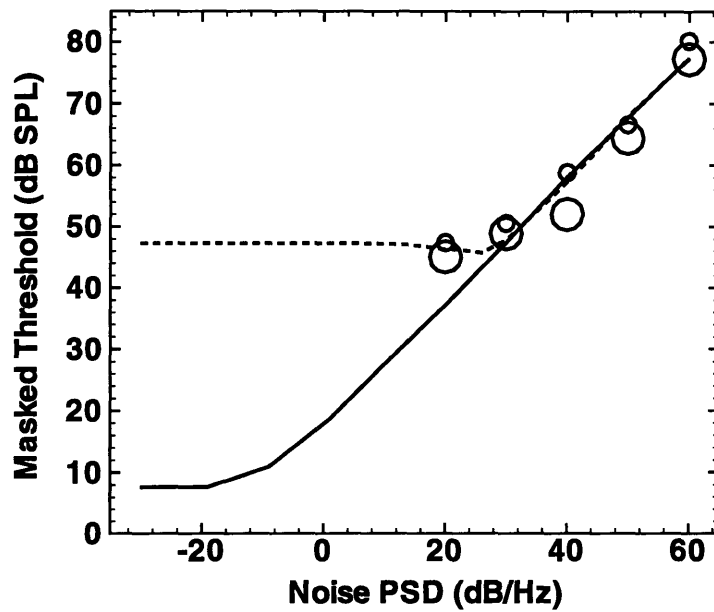


Figure 5-13: Filterbank effects of changing the probe frequency in the expansion simulated condition for subject KL. Symbol size increases as the frequency increases from the edge of the band (955 Hz) to nearer the center (1000 Hz).

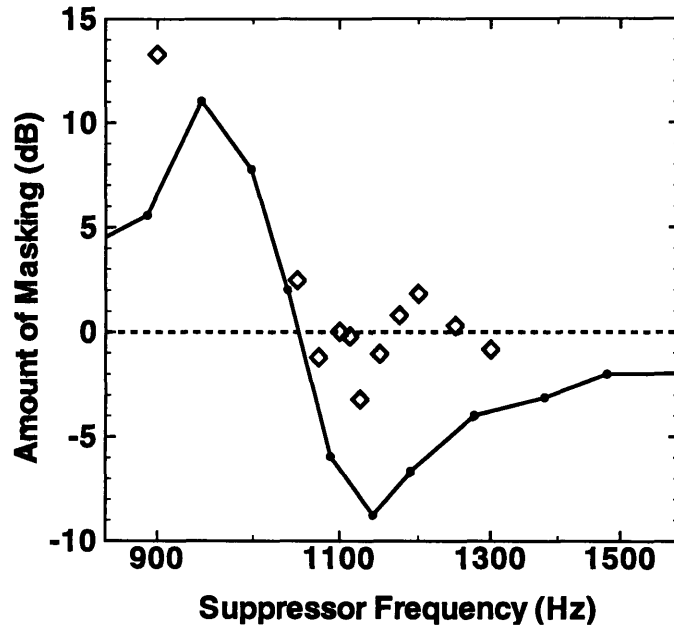


Figure 5-14: Data from the unsimulated condition of the suppression experiments ( $\diamond$ ) shown with data from Shannon (solid line). Probe tone was at 1000 Hz. Each data point measures the amount of masking as a function of suppressor frequency, so that negative values indicate suppression. The threshold for the probe tone with no suppressor present (i.e. 0 dB of masking) was 30.7 dB SPL.

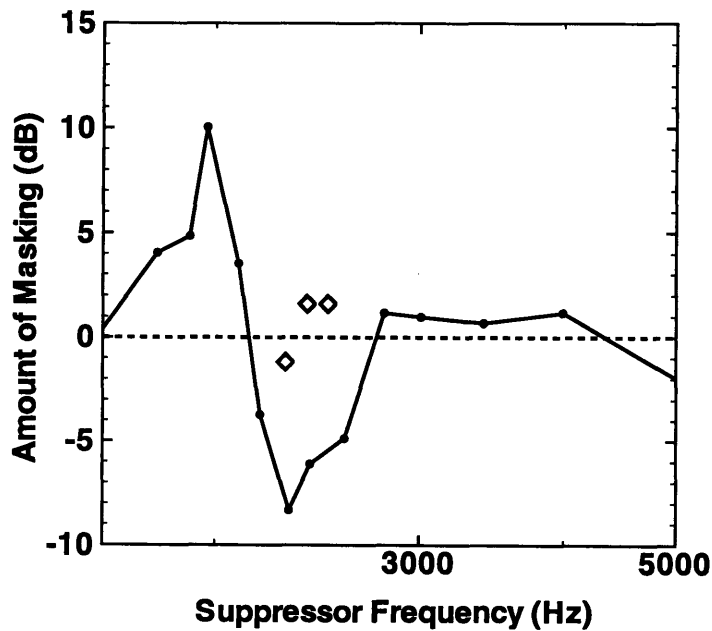


Figure 5-15: Identical to Figure 5-14, except that the probe tone was at 2000 Hz. The threshold for this probe with no suppressor present (i.e. 0 dB of masking) was 32.4 dB SPL.

simulated experiments were not performed.

# Chapter 6

## Discussion

### 6.1 Intensity Discrimination

In general the predictions and experimental data for intensity discrimination are in agreement: the data points in the expansion simulated conditions come to a sharp peak as the overall level increases, and sensitivity is *always* better than normal. Table 6.1 summarizes the effects of the two hearing loss simulations by reporting whether they provided better or worse than normal sensitivity when compared with the unsimulated condition at equal sound pressure, equal sensation level, and equal loudness. The table also includes the effects of a real flat hearing loss from Florentine et al. [9]. The expansion simulator provides better than normal sensitivity no matter how the comparison is made. The noise simulation causes both improvements *and* reductions in sensitivity, depending on how the comparison is made. At equal sound pressure levels, noise simulation reduces sensitivity; at equal sensation levels (at least above 20 dB SL) it *increases* sensitivity; and at equal loudness there is no clear trend.

When the the results of the simulations are compared to those of a real impairment, it becomes obvious that the noise simulation is the better performer. Florentine et al. have shown that hearing impaired persons possess sensitivity comparable to or worse than normal hearing persons when

	Expansion	Noise	Impairment
Equal SPL	+	-	-
Equal SL	+	+	+
Equal loudness	+		-

Table 6.1: Effect of the two hearing loss simulations and real impairment on intensity discrimination when compared with normal data at equal sound pressure levels, equal sensation levels, and equal loudness. A “+” indicates *better than normal* sensitivity, a “-” indicates *worse than normal* sensitivity, and the absence of a symbol means that the results were ambiguous. Impaired data was taken from Florentine et al.’s “flat audiograms.”

compared at equal sound pressure levels and loudness. When compared at equal sensation levels, impaired subjects have sensitivity comparable to or better than normal. The symbols in Table 6.1 clearly indicate that the noise simulation results match real impairments more closely than the expansion simulation, which always *increases* sensitivity.

In the expansion simulated condition, comparing with the unsimulated case at equal loudness is actually comparing at equal *headphone* levels. Comparing in this way nullifies the simulator's attenuating property and allows the expansive property to have its full impact. The average experimental improvement afforded by the expansion simulator at equal headphone levels was a factor of 3.0, which is close to the system's expansion factor (2.67) for a 50 dB loss. This result supports our treatment of 400 ms tones as infinite duration sinusoids which are ideally expanded by the simulator.

## 6.2 Psychoacoustic Tuning Curves

The expansion simulated prediction of DL's tuning curves in Figure 5-7 appear visually better than the prediction of AM's data in Figure 5-8. The reason is probably that Nelson's data on normal hearing subjects could be shifted to fit DL's *unsimulated* tuning curve much more closely than AM's. The average magnitude of error between the *unsimulated* data points and the fitted Nelson data was 5.3 dB for DL but 13.9 dB for AM, mainly because AM's curve was narrower than both the Nelson data and DL's. In other words, the assumed model of normal hearing was a good one for DL but a poor one for AM.

Not surprisingly, the PTCs predicted for the expansion simulated case fit DL's experimental data more closely than AM: the average magnitude of error was 6.3 dB for DL and 7.4 dB for AM. The difference in accuracy is not nearly so great as the difference in the unsimulated case, suggesting that AM's unusually narrow PTC did not survive the process of hearing loss simulation.

Qualitatively the experimental data agrees very well with the predictions. The tuning curves from both the expansion and noise simulations are higher and broader than the unsimulated tuning curves. Real hearing impairment also tends to decrease frequency selectivity and broaden out the shape of PTCs, as shown by the data of Dubno and Schaefer [4]. For the expansion simulator, there are two underlying causes of the broadening, as explained in Section 4.2. One of them has to do with elevated probe levels, but the other is inherent in the expansion property of the simulator.

## 6.3 Simultaneous Masking

For the unsimulated condition of the simultaneous masking experiment, the agreement between the predicted masked thresholds (from the Hawkins and Stevens data) and the experimental ones was very good. The only discrepancies are for the highest noise level (60 dB/Hz); the threshold at this

level was consistently higher than expected for all three subject by about 2–4 dB. One explanation for this is that bursts of noise at such a high level were unpleasantly loud for the subjects and caused greater difficulty in detecting the tone than the signal-to-noise ratio would account for. JW especially complained about the loudness of the noise at 60 dB/Hz.

The two hearing loss simulations will be discussed separately, beginning with the noise simulation. For KL the results are unsurprising. Masked threshold does not deviate far from the unsimulated case for the higher noise levels (30–60 dB/Hz), where the effect of the additive noise used to simulated hearing loss is drowned out by the much more powerful broadband masking noise. Only when the masking noise drops below the level of the additive simulation noise (i.e. at 20 dB/Hz) do the results diverge from the unsimulated case. The masked threshold *must* stay above the impaired threshold, which has been placed near 48 dB SPL by equivalent threshold masking.

For JW in the noise simulated condition, the masked thresholds rise above the unsimulated results. At low masker levels (e.g. 20, 30 dB/Hz) an explanation for this is that the noise wasn't carefully enough controlled and actually raised the subject's threshold by more than 40 dB. At suprathreshold masker levels (40, 50 dB/Hz) this explanation doesn't apply; the discrepancy of  $\sim 4$  dB at the 40 dB/Hz level is unexplained.

In the expansion simulation the masked thresholds at suprathreshold masker levels are generally *lower* than the predictions, except at the 60 dB/Hz level. At this level the thresholds matched the unsimulated results for all subjects; this makes sense, because at this high level the simulator is operating above the threshold of complete recruitment, essentially having no effect on the signal. At the *other* suprathreshold masker levels (40, 50 dB/Hz) the masked thresholds are lower than normal by an average of 2.5 dB for JW and 5.5 dB for KL. For JL there is essentially no difference in the expansion simulated and unsimulated conditions for suprathreshold maskers.

The expansion simulated results were baffling until it was suggested that perhaps the subjects had been basing their decisions on an unforeseen cue: changes in noise level. In the masked threshold experiment, the subjects were presented two intervals of noise and asked to identify the one which had *also* contained a tone burst. However, in the expansion simulated case (unlike the other two cases) the presence of a tone could actually *amplify* the level of the noise masker above its level in isolation. A specific example is given: suppose that two intervals of noise at 40 dB/Hz are presented and the second one also contains a 1 kHz tone burst at normal masked threshold (60 dB SPL). Assume that the expansion simulator is simulating a loss of 40 dB so that the slope  $K$  of its input/output relation is 2.15. In the first noise burst, the simulator will measure 64.3 dB total power in the bandpass filter spanning the 941–1074 Hz range. In the second burst of tone+noise, the simulator will measure 65.7 dB total power in that filter. Given the input/output function of Figure 1-3, this difference of 1.4 dB between the two interval levels means that the first interval will receive  $1.4(K - 1) = 1.6$  dB *more attenuation* from the system than the second one will. Therefore,

it is possible that the subject could base his decision *not* on the question “which interval contained the tone?” but instead on the question “which interval of noise sounded louder?”

If it is assumed that a subject can perceive a difference in noise intensity of 1 dB, then he will be able to use this alternate cue until the addition of the tone results in less than 1 dB of change in the amount of attenuation applied to the noise. To uphold this condition in the example above, the tone level must be reduced to 57.8 dB SPL, which is a reduction of 2.2 dB from the original masked threshold. If the subject possesses even *greater* sensitivity to differences in noise intensity (e.g. 0.5 dB) then the reduction in masked threshold would increase to 6.5 dB. These arguments may explain why KL and JW exhibited a reduction in masked thresholds in the expansion simulated condition on the order of 3–5 dB. It must be assumed that JL (who did not display reduced thresholds) did not use this alternate cue to make his decisions.

The effects of the expansion simulator’s bandpass nature are investigated in Figures 5-12 and 5-13 by plotting masked threshold at various frequencies near the edge of the 941–1206 Hz filter (945 Hz, 955 Hz) and near the center (1000 Hz). For JW there was no frequency-related trend to the data. For KL, every masked threshold at 955 Hz was several dB above the corresponding one at 1000 Hz, with an average difference of 3.2 dB. This result is contradictory to the filterbank effects predicted by Section 4.3, which predicted a *higher* SNR for frequencies near the edges, and thus *lower* masked thresholds. One possible explanation is valid if KL had become dependent on the change in noise loudness as a cue and had stopped depending on detecting the actual tone. As the probe tone nears the edge of one of the simulator filters, only half of the spectrum entering the ear comes from the filter which is affected by the introduction of the tone; consequently, the introduction of the tone has less effect on the total amount noise entering the ear. The reduced effectiveness of KL’s alternate cue could raise his threshold, although calculations do not predict an effect as large as 3 dB.

Dubno and Schaefer have shown that there is essentially no correlation between critical ratio and impaired threshold for 21 impaired subjects. An analogous demonstration for the simulated impaired subjects in this thesis would be to show that the hearing loss simulations do not cause significant changes in masked threshold for suprathreshold stimuli. Although it is hard to prove significance with so few data points, some arguments can be made. For subjects JW, KL, and JL, the expansion simulated masked threshold was lower than in the unsimulated condition in 6 out of 10 suprathreshold cases. For JW and KL, the noise simulated masked threshold was higher than the unsimulated condition in 4 out of 6 suprathreshold cases. Neither of these results appears to be a significant change, suggesting that the results of the simulated impaired subjects resemble the results of Dubno and Schaefer’s real impaired subjects.



# Chapter 7

## Conclusion

The fundamental goal of further characterizing the effects of expansion simulation of hearing loss has been achieved. The experimental results of this thesis begin to fill in previously empty spaces in Table 7.1, which lists two methods of simulating hearing loss as well as sources which have characterized them. The table is by no means a complete listing of all of the research on equivalent threshold noise masking; however, it does cite most of the experiments which have been performed using both kinds of simulations.

Since the data in this thesis was gathered using both kinds of hearing loss simulation, their effectiveness in reproducing the effects of a real loss could be compared. In addition to providing a more complete description of the expansion simulator's effects, the experiments have also yielded information about the system's limitations and artifacts.

### Comparison of Simulations

A major advantage of noise simulation of hearing loss is ease of implementation. To achieve equivalent threshold noise masking requires only a white noise generator and a filterbank; to achieve real-time dynamic amplitude expansion requires special analog or DSP hardware. However, one

	Noise Simulation	Expansion Simulation
<b>Speech Stimuli</b>		
<i>CVs</i>	Zurek and Delhorne [29]	Duchnowski [5]
<i>Sentences</i>	DeGennaro [3]	Duchnowski [5]
<b>Traditional Stimuli</b>		
<i>Intensity Discrimination</i>	Florentine et al. [9]	<i>this thesis</i>
<i>PTCs</i>	Dubno and Schaefer [4]	<i>this thesis</i> and Lum [14]
<i>Critical Ratio</i>	Dubno and Schaefer [4]	<i>this thesis</i>
<i>Narrow band Masking</i>	Dubno and Schaefer [4]	Lum [14]

Table 7.1: Some existing sources to characterize the simulation of hearing loss.

major advantage of expansion simulation is perceptual realism. Persons with hearing impairment do not experience constant noise. Also, expansion simulations can be used to simulated severe hearing losses; to do so with additive noise would require intolerably high noise levels.

In the experiment to measure psychoacoustic tuning curves, both the expansion and noise simulations produce results which qualitatively match the broadened tuning curves of a real impairment [4]. Such results have not been measured before with an expansion simulation. They are somewhat surprising, because reduced frequency selectivity (as measured by PTCs) was *not* explicitly built into the system; only elevated thresholds and abnormal loudness growth was. These results suggest that those two effects of hearing loss *alone* necessarily produce a reduction in frequency selectivity.

In the intensity discrimination experiment, the expansion and noise simulations produce markedly different results. The expansion simulation gives a normal hearing person better than normal sensitivity when compared at equal SPL, SL, or loudness. In contrast, the noise simulation *decreases* a person's normal sensitivity when compared at equal SPL, has no effect when compared at equal loudness, and may increase sensitivity when compared at equal SL. Of the two simulations, only additive noise produces effects which resemble the effects of real impairment [9]. The enhanced intensity discrimination afforded by the expansion simulation is not a desired effect.

In the experiment to measure masked thresholds in broadband noise, the expansion and noise simulations again have similar effects. Neither simulation appears to significantly raise or lower masked threshold in the presence of suprathreshold masking noise; consequently, neither has a significant effect on critical ratios. These results match the results from real impairments, which show essentially no correlation between degree of impairment and critical ratio [4].

## Limitations of the Expansion Simulation

One limitation of the expansion simulator is that, in order to simulate the effects of recruitment, it must also enhance the intensity discrimination of the normal hearing person using it. This undesired effect is an *artifact* of the implementation.

Another artifact was demonstrated in Figure 4-13, which shows the predictions of masked thresholds in noise. At the more severe hearing losses (40, 50 dB) there is a section of the masked threshold function which clearly dips *below* absolute threshold by 2 or 3 dB. The explanation for this artifact is as follows: in the expansion simulation, the addition of a second input sound to an existing one will raise the *output* level of the existing sound. The models in Section 4.3 predict that a *subthreshold* probe tone can be raised *above* threshold by the addition of a small amount of noise which is not enough to mask it. There is no physiological reason to expect this result in real impaired subjects, but the expansion simulated data from JW in Figure 5-9 may support the prediction of this artifact: at the 30 dB/Hz noise level, JW's masked threshold is several dB below absolute threshold. However, one data point does not prove a theory, and there are further complications in interpreting the

simultaneous masking data as described in Section 6.3.

A lesson to be learned from this thesis is that great care must be taken when designing psychoacoustic experiments to be performed with expansion simulation. Because the presence of one input can have a large effect on the output level of a second, additive stimuli are no longer *independent* as they are in the unsimulated condition. In particular, the assumption that was used in the simultaneous masking experiment was that the *only* parameter that was different in the two presentation intervals was the presence of the probe tone. More careful thought revealed that the level of the *masking noise* was also changed by the introduction of the tone, providing the subject with another cue on which to base his decision. This sort of problem will be a factor in any experiment which involves the simultaneous presentation of two or more sounds. It was not a problem in the intensity discrimination and tuning curve experiments, because at no point in those experiments was more than one sound presented at the same time.

## Future Work

Several possibilities for future work with the expansion simulation include: experimenting with amplitude compression systems (hearing aids) to see how successfully they can reverse the simulator's detrimental effects; investigating different static input/output relations<sup>1</sup> to see if the artifact of enhanced intensity discrimination can be eliminated; and performing additional psychoacoustic experiments to further characterize the system. Two tone suppression would be interesting to study if normal hearing subjects who exhibit it can be found.

---

<sup>1</sup>The piecewise linear function in Figure 1-3 is only an approximation to measured equal-loudness functions such as those in Miskolczy-Fodor [16]. Other shapes have been proposed and discussed [11],[25].

## Appendix A

# Derivation of Sensitivity-per-Bel Measures from Experimental Data

This appendix describes the process by which the data from the intensity discrimination experiments was transformed into units of sensitivity-per-Bel. The data points gathered in the experiment relate the difference in intensity of two tone bursts to the percentage of correct identifications (out of 40 trials) of the louder one. Figures A-1, A-2, and A-3 present the data from three subjects.

An established method of modelling a subject's performance in a 2AFC intensity discrimination experiment is presented by Durlach [6]. Let the intensities of the soft and loud tone bursts be  $I$  and  $I + \Delta I$ , respectively. It is assumed that the loud and soft tones are perceived as random variables defined on a one-dimensional decision space,  $d_0$ , with probability density functions  $f_L(d_0)$  and  $f_S(d_0)$ , respectively. Both densities are assumed to be unit normal functions whose means are separated by the amount  $d'$ . Since the position of the densities on the  $d_0$  axis is arbitrary,  $f_S(d_0)$  will be placed at the origin so that

$$f_S(d_0) = \frac{1}{\sqrt{2\pi}} \exp\left(\frac{-d_0^2}{2}\right) \quad \text{and} \quad f_L(d_0) = \frac{1}{\sqrt{2\pi}} \exp\left(\frac{-(d_0 - d')^2}{2}\right).$$

The decision space is portrayed graphically in Figure A-4.

With equal probability, the subject is presented with the sequence (loud, soft) or (soft, loud), producing the pair of random variables  $(X_1, X_2)$ ; he is asked to identify the louder tone. It is assumed that the subject bases his decision on the decision variable  $Y = X_1 - X_2$ , which has variance 2 and mean  $\pm \frac{d'}{2}$ , depending on whether the order of presentation was (loud, soft) or (soft, loud). The two conditional densities of  $Y$  are shown in Figure A-5 and expressed in the equations:

$$f_{Y|L,S}(Y_0) = \frac{1}{\sqrt{4\pi}} \exp\left(\frac{-(Y_0 - \frac{d'}{2})^2}{4}\right) \quad \text{and} \quad f_{Y|S,L}(Y_0) = \frac{1}{\sqrt{4\pi}} \exp\left(\frac{-(Y_0 + \frac{d'}{2})^2}{4}\right).$$

To minimize the probability of error, the subject responds "loud, soft" when  $Y > 0$  and "soft, loud"

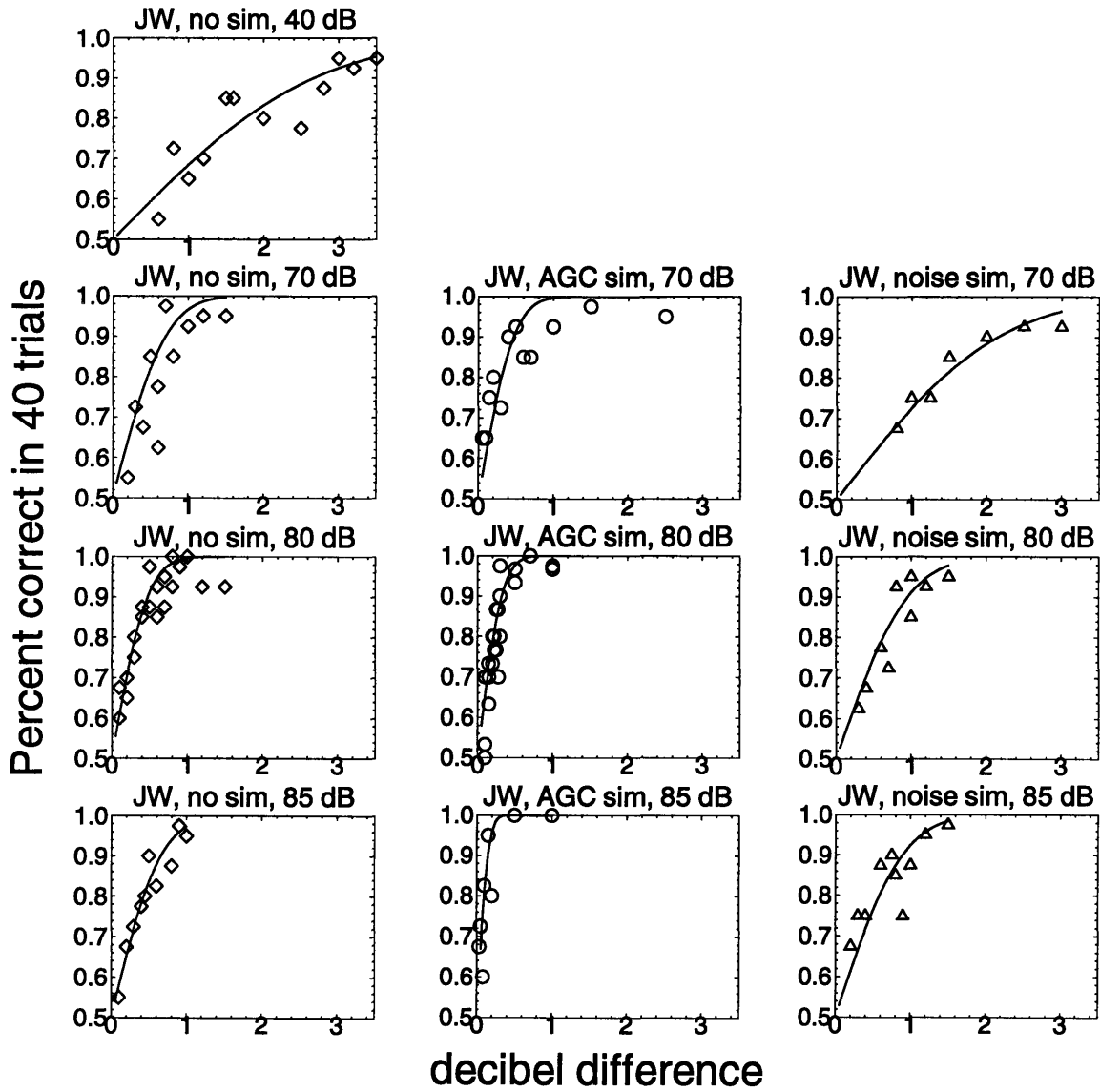


Figure A-1: Data from the intensity discrimination experiment for subject JW. Data points are shown for the unsimulated case ( $\diamond$ ), the expansion simulated case ( $\circ$ ), and the noise simulated case ( $\triangle$ ). Solid lines are the best-fit sigmoid through the data points. Overall sound levels are indicated at the top of each panel.

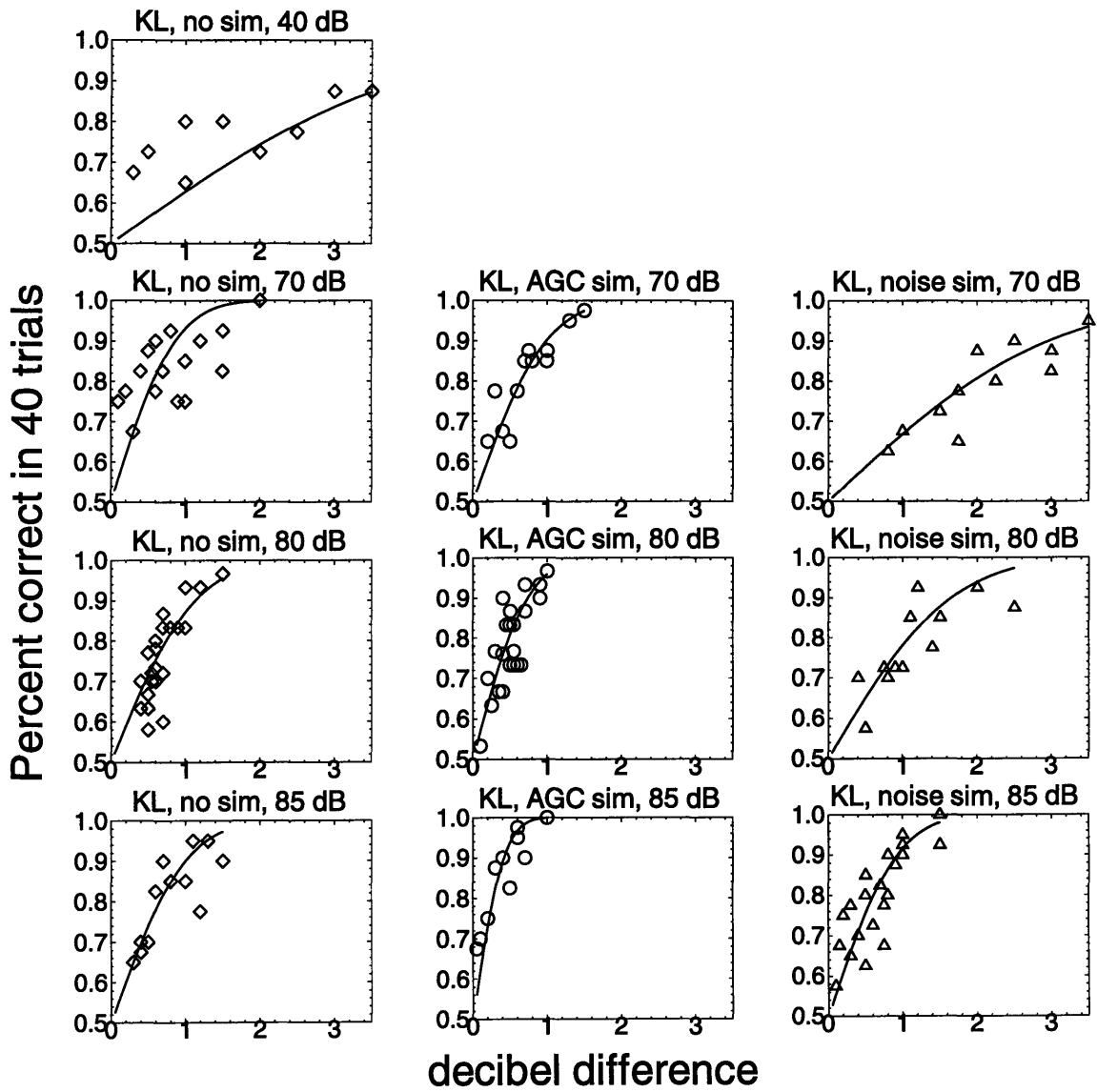


Figure A-2: Data for subject KL. Legend is identical to Figure A-1.

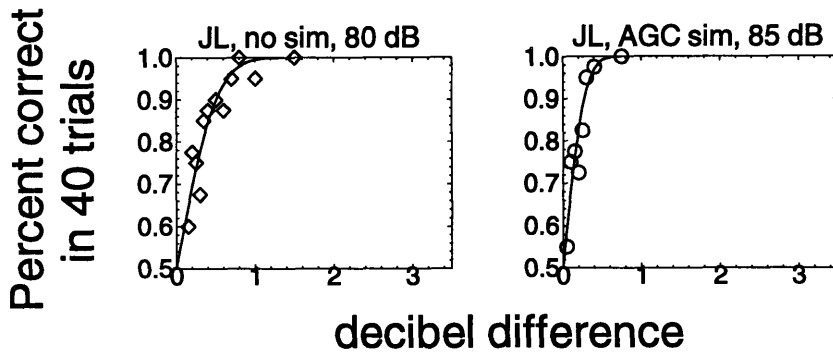


Figure A-3: Data for subject JL. Legend is identical to Figure A-1, except that fewer experimental conditions were examined.

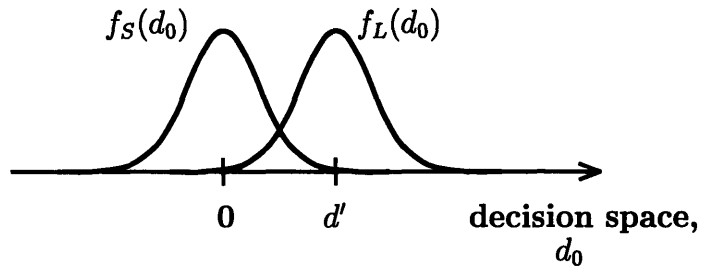


Figure A-4: Decision space for the 2AFC intensity discrimination experiment.

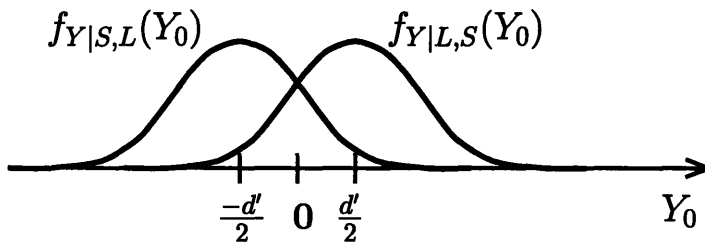


Figure A-5: Conditional probability densities for the difference of the two observations  $X_1$  and  $X_2$ .

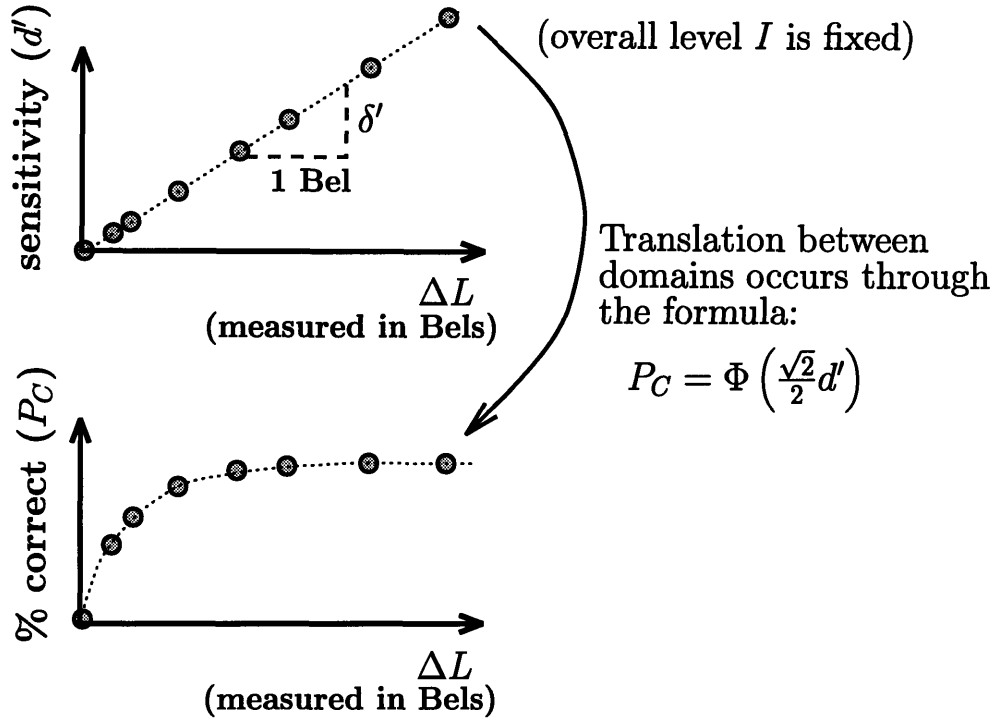


Figure A-6: The two domains of the intensity discrimination experiment. In the “percent correct domain,” the function relating Bel intensity difference to percent correct is a sigmoid. In the “ $d'$  domain,” the function relating Bel intensity difference to  $d'$  is a straight line through the origin with slope  $\delta'$ . Translations are made between domains by means of Equation A.1.

when  $Y < 0$ .

With this model in place, the probability of a correct response becomes

$$\text{Prob}(\text{correct}) \equiv P_C = \text{Prob}(L, S) \cdot \text{Prob}(Y > 0 | L, S) + \text{Prob}(S, L) \cdot \text{Prob}(Y < 0 | S, L)$$

which evaluates to

$$P_C = \frac{1}{2} \left[ \Phi\left(\frac{\sqrt{2}d'}{2}\right) + \Phi\left(\frac{\sqrt{2}d'}{2}\right) \right]$$

or

$$P_C = \Phi\left(\frac{\sqrt{2}d'}{2}\right), \tag{A.1}$$

where the function  $\Phi(\cdot)$  is the cumulative distribution function of the zero-mean unit normal, i.e.

$$\Phi(x) = \int_{-\infty}^x \frac{1}{\sqrt{2\pi}} \exp\left(-\frac{x_0^2}{2}\right) dx_0.$$

The quantity  $d'$ , being the separation of the means of two Gaussians, is a measure of the subject's *sensitivity*. As the experimental parameters  $I$  and  $\Delta I$  are changed, the sensitivity also changes:  $d'$  is actually the function  $d'(I, I + \Delta I)$ . Following Rabinowitz et al., it is assumed that at a given overall level  $I$  the dependence of  $d'(I, I + \Delta I)$  on  $\log\left(\frac{I + \Delta I}{I}\right)$  is *linear* and passes through the origin.



Intensity discrimination is defined as the slope of that line, which has units of *sensitivity-per-Bel* and is given the symbol  $\delta'$ . The relationships between percent correct ( $P_C$ ),  $d'$ , and  $\delta'$  are graphically shown in Figure A-6, where  $\Delta L = \log\left(\frac{I+\Delta I}{I}\right)$ .

For each overall intensity  $I$ , a set of data points relating  $\Delta L$  to  $P_C$  was obtained experimentally; this is the data presented in Figures A-1, A-2, and A-3. Values of  $\delta'$  were searched to find the one which produced the best-fitting set of  $P_C$ s using the experimental  $\Delta L$ s and the equation:

$$P_C = \Phi\left(\frac{\sqrt{2}\delta'\Delta L}{2}\right).$$

The resulting  $\delta'$  was used to generate the best-fit sigmoids shown in the figures as well as the single data points presented in Section 5.1. The error criterion used in fitting was total summed magnitude of error.

To take into account the fact that estimates of  $P_C$  are more accurate near 100% than near 50%, the error contributions were weighted. The weighting was a division by the variance of the random variable

$$\hat{P}_C = \frac{k}{40},$$

which makes an estimate of the true  $P_C$  by dividing the number of correct trials by the total number of trials. The variance of this estimator is

$$\text{Var}(\hat{P}_C) = \frac{P_C(1 - P_C)}{40},$$

but was clipped to  $\frac{1}{40} \cdot \frac{39}{40} \left(1 - \frac{39}{40}\right)$  for experimental values of  $P_C$  equal to 1.0 to avoid dividing by zero.

# Bibliography

- [1] Specifications for audiometers. Technical report, American National Standards Institute, New York, 1970.
- [2] *User's Manual for the DSP-96 DSP96002 Floating-Point Attached Processor Board with Dual-Channel Analog I/O*. Ariel Corporation, Highland Park, NJ, 1993.
- [3] Steven Vincent DeGennaro. The effect of syllabic compression on speech intelligibility for normal listeners with simulated sensorineural hearing loss. Master's thesis, Massachusetts Institute of Technology, Cambridge, MA, 1978.
- [4] Judy R. Dubno and Amy B. Schaefer. Frequency selectivity for hearing-impaired and broadband-noise-masked normal listeners. *The Quarterly Journal of Experimental Psychology*, 43A(3):543–564, 1991.
- [5] Paul Duchnowski. Simulation of sensorineural hearing impairment. Master's thesis, Massachusetts Institute of Technology, Cambridge, MA, 1989.
- [6] Nathaniel I. Durlach. A decision model for psychophysics. MIT Research Laboratory of Electronics Sensory Communication Group, 1968.
- [7] E.F. Evans and J. P. Wilson, editors. *Psychophysics and Physiology of Hearing*. Academic, London, 1977.
- [8] H. Fletcher. Auditory patterns. *Reviews in Modern Physics*, 12:47–61, 1940.
- [9] Mary Florentine, C. M. Reed, W. M. Rabinowitz, L. D. Braida, and N. I. Durlach. Intensity perception. xiv. intensity discrimination in listeners with sensorineural hearing loss. *The Journal of the Acoustical Society of America*, 94(5):2575–2586, 1993.
- [10] Donald D. Greenwood. Auditory masking and the critical band. *The Journal of the Acoustical Society of America*, 33(4):484–502, 1961.
- [11] C.S. Hallpike and J. D. Hood. Observations upon the neurological mechanism of the loudness recruitment phenomenon. *Acta Oto-laryngologica*, 50:472–486, 1959.

- [12] J.E. Hawkins Jr. and S. S. Stevens. The masking of pure tones and speech by white noise. *The Journal of the Acoustical Society of America*, 22(6), 1950.
- [13] M. Charles Liberman and Leslie W. Dodds. Single-neuron labeling and chronic cochlear pathology. iii. stereocilia damage and alterations of threshold tuning curves. *Hearing Research*, 16:55–74, 1984.
- [14] David Lum. Evaluation of a hearing loss simulator. Advanced Undergraduate Project, Massachusetts Institute of Technology, Cambridge, MA, 1994.
- [15] David S. Lum. Description of the combination simulatr/mod software. MIT Research Laboratory of Electronics Sensory Communication Group, 1995.
- [16] F. Miskolczy-Fodor. Relation between loudness and duration of tonal pulses. iii. response in cases of abnormal loudness function. *The Journal of the Acoustical Society of America*, 32(4):486–492, 1960.
- [17] David A. Nelson, Steven J. Chargo, Judy G. Kopun, and Richard L. Freyman. Effects of stimulus level on forward-masked psychophysical tuning curves. *The Journal of the Acoustical Society of America*, 88(5):2143–2151, November 1990.
- [18] Roy D. Patterson. Auditory filter shape. *The Journal of the Acoustical Society of America*, 55(4):802–809, April 1974.
- [19] Roy D. Patterson and G. Bruce Henning. Stimulus variability and auditory filter shape. *The Journal of the Acoustical Society of America*, 62(3):649–664, September 1977.
- [20] Patrick M. Peterson and Joseph A. Frisbie. An interactive environment for signal processing on a vax computer. *Proceedings of ICASSP*, pages 1891–1894, April 1987.
- [21] James O. Pickles. *An Introduction to the Physiology of Hearing*. Academic Press, London, second edition, 1988.
- [22] W.M. Rabinowitz, J.S. Lim, L.D. Braida, and N.I. Durlach. Intensity perception vi. summary of of recent data on deviations from Weber’s law for 1000-Hz tone pulses. *The Journal of the Acoustical Society of America*, 59:1506–1509, 1976.
- [23] R.V. Shannon. Two-tone unmasking and suppression in a forward-masking situation. *The Journal of the Acoustical Society of America*, 59:1460–1470, 1976.
- [24] S. S. Stevens, editor. *Handbook of Experimental Psychology*. Wiley, New York, 1951.
- [25] S.S. Stevens. Power-group transformations under glare, masking, and recruitment. *The Journal of the Acoustical Society of America*, 39(4):725–735, 1966.

- [26] Dianne J. Van Tasell. Hearing loss, speech, and hearing aids. *Journal of Speech and Hearing*, 36:228–244, April 1993.
- [27] M. M. Taylor and C. Douglas Creelman. PEST: Efficient estimates on probability functions. *The Journal of the Acoustical Society of America*, 41(4, Part 1):782–787, April 1967.
- [28] Edgar Villchur. Simulation of the effect of recruitment on loudness relationships in speech. *The Journal of the Acoustical Society of America*, 56(5):1601–1611, November 1974.
- [29] P. M. Zurek and L. A. Delhorne. Consonant reception in noise by listeners with mild and moderate sensorineural hearing impairment. *The Journal of the Acoustical Society of America*, 82(5):1548–1559, November 1987.

7103-39